

UNCLASSIFIED

AD **407 921**

DEFENSE DOCUMENTATION CENTER

FOR

SCIENTIFIC AND TECHNICAL INFORMATION

CAMERON STATION, ALEXANDRIA, VIRGINIA



UNCLASSIFIED

NOTICE: When government or other drawings, specifications or other data are used for any purpose other than in connection with a definitely related government procurement operation, the U. S. Government thereby incurs no responsibility, nor any obligation whatsoever; and the fact that the Government may have formulated, furnished, or in any way supplied the said drawings, specifications, or other data is not to be regarded by implication or otherwise as in any manner licensing the holder or any other person or corporation, or conveying any rights or permission to manufacture, use or sell any patented invention that may in any way be related thereto.

R63-16

DASA-1373

DEPARTMENT OF CIVIL ENGINEERING
EVALUATION OF MODEL TECHNIQUES FOR THE INVESTIGATION
OF STRUCTURAL RESPONSE TO BLAST LOADS

Harold D. Smith
Robert W. Clark
Richard P. Mayor

Supervised by
Robert J. Hansen

February, 1963

This research was supported by the
DEFENSE ATOMIC SUPPORT AGENCY

NWER Subtask 13.106

Contract DA-49-146-XA-093
DSR 8839

Reproduction in whole or in part is permitted for any
purpose in the United States Government

School of Engineering
MASSACHUSETTS INSTITUTE OF TECHNOLOGY
Cambridge 39, Massachusetts

TABLE OF CONTENTS

	Page
CHAPTER 1 INTRODUCTION	
1.1 Objectives	1
1.2 Background	2
CHAPTER 2 SIMILITUDE	
2.1 General	3
CHAPTER 3 PROCEDURE	
3.1 Prototype	
3.1.1 Prototype Selection	6
3.1.2 Prototype Dimensions	6
3.1.3 Material Properties	6
3.2 Domes	
3.2.1 Geometric Scaling	7
3.2.2 Fabrication	7
3.2.3 Casting	8
3.2.4 Properties of the Model Materials	9
3.3 Model Testing Procedure	12
3.4 Charge Scaling	13
3.5 Instrumentation	13
CHAPTER 4 DYNAMIC TEST RESULTS	30
CHAPTER 5 SIGNIFICANCE OF DURATION TIME SCALING	
5.1 Introduction	40
5.2 Procedure	
5.2.1 General	40
5.2.2 Load	40
5.2.3 Dynamic Response	41
5.2.4 Capacity	41
5.3 Results	43
5.4 Effect of Duration Time	44

TABLE OF CONTENTS (Cont'd.)

	Page
CHAPTER 6 STATIC TESTS ON MODEL DOME STRUCTURES	
6.1 Introduction	48
6.2 Loading Pattern	48
6.3 Loading System	48
6.4 Loading Frame	48
6.5 Instrumentation	49
6.6 Test Procedure	49
6.7 Results of Static Dome Tests	50
6.8 Conclusions	51
CHAPTER 7 CONCLUSIONS	59
REFERENCES	61

LIST OF FIGURES

	Page
Figure 3.1 Dome Reinforcement Placing	14
3.2 Prototype Dome - 20 psi	15
3.3 Prototype Dome - 35 psi	15
3.4 Prototype Dome - 70 psi	16
3.5 Prototype Concrete Strength	17
3.6 Mesh Fabrication	18
3.7 Reinforcing Mesh	18
3.8 Model Aggregate Size Distribution	19
3.9 Lower Mesh on Casting Form	20
3.10 Thickness Scriber	20
3.11 Part Section Through Dome Model Showing Base Ring	21
3.12 Stress-Strain Curve of Model Reinforcing Wire	22
3.13 Mortar Strength vs. Age	23
3.14 Some Mortar Stress-Strain Curves	24
3.15 Some Mortar Stress-Strain Curves	25
3.16 Some Mortar Stress-Strain Curves	26
3.17 View of Model Installations Loading Away from Zero	27
3.18 Predicted and Measured Overpressure versus Distance for a 100 - Ton TNT Surface Burst	28
3.19 Predicted and Measured Positive Duration versus Distance for a 100-Ton TNT Surface Burst	29
4.1 80 psi Dome Preshot	31
4.2 80 psi Dome Postshot	31
4.3 70 psi Dome Preshot	32
4.4 70 psi Dome Postshot	32
4.5 60 psi Dome Preshot	33
4.6 60 psi Dome Postshot	33
4.7 40 psi Dome Preshot	34
4.8 40 psi Dome Postshot	34

LIST OF FIGURES (Cont'd.)

		Page
Figure	4.9 40 psi Dome Preshot	35
	4.10 40 psi Dome Postshot	35
	4.11 40 psi Dome Preshot	36
	4.12 35 psi Dome Postshot (note missile damage)	36
	4.13 35 psi Dome Preshot	37
	4.14 35 psi Dome Postshot	37
	4.15 30 psi Dome Preshot	38
	4.16 30 psi Dome Postshot	38
	4.17 20 psi Dome Postshot	39
	5.1 Effects of Duration Time on Model Behavior	46
	5.2 Pressure-Time Curve for Typical Point on Model	47
	6.1 Discrete Load Locations	53
	6.2 Loading System	54
	6.3 Loading System	55
	6.4 Test Frame	56
	6.5 Test Frame with Model and Loading System	57
	6.6 Collapsed Model, ND1	58

LIST OF TABLES

	Page
TABLE 1.1 Microconcrete Strength	10
6.1 Static Failure Pressures of the Model Domes	50
6.2 Evaluation of Test Results	52

ABSTRACT

The objective of this investigation was to evaluate the study of structural response to dynamic loads through the use of structural models and to evaluate the related modeling techniques.

The responding domes of Operation Plumbbob were modeled at one twenty-fifth scale using mild steel wire and microconcrete. These models were field tested under blast wave loading conditions at overpressures ranging from 80 psi to 20 psi.

Good agreement was obtained between model and prototype structure in both failure mechanism and appearance, as well as in the location of the failure-survival pressures.

It is concluded that with proper compliance with the similitude laws and adequately accurate fabrication techniques the modeling of the response of structures to dynamic loads can be quite successful.

CHAPTER 1

INTRODUCTION

1.1 OBJECTIVES

The objective of this investigation is to provide a basis for evaluation of the modeling techniques involved in dynamic structural studies. This is desirable for the following reasons.

At present the United States of America is involved in an extensive program of design and construction of hardened facilities. These structures vary from the simpler more easily analysed types to very complex forms requiring many assumptions for analytical treatment. Pressure levels of interest vary from a few pounds per square inch to many hundreds. Structural types also range from above-ground to completely buried. Thus experimental work is necessary so that these varied types of structures can be designed to most economically possess the required strength.

In the past, most field investigations have been carried out at full scale under nuclear blast conditions. This has several disadvantages. The prototype structures are very costly due to their site location and related labor and material conditions. Also the uncertainty of nuclear testing as influenced by political and economic factors is a consideration. These factors contribute to the desirability of using models in dynamic structural studies.

A dynamic model technique if properly executed offers the potential of (a) developing further basic information such as loading functions, and behavioral and failure models of structural systems, and (b) the evaluation of specific designs. The possibility of modeling complex structures permits the use of loading systems other than a nuclear device.

The direct objective of project US-16 in the 1961 Canadian 100-ton TNT trial is to evaluate the reliability of the modeling technique by checking a model experiment against a previously performed full scale nuclear experiment.

1.2 BACKGROUND

Experimental investigations have been used since the ancient beginnings of construction. Although at first these were in effect the construction of the prototype itself, man soon found it advantageous to perform studies at a "small" scale and, after acquiring an understanding of the physical behavior involved, to later create the prototype based upon the new and more thorough knowledge.

Engineering fields have grown through the use of experimental studies to either validate or refute physical behavior hypotheses. Early work in the field of structures assumed linearly elastic behavior of materials. Because of the linear nature of these problems much flexibility was permitted in the selection of the modeling parameters. In general, any linearly elastic material can be selected if other factors such as the magnitude of the test loads do not rule out its use.

Recently, the need for economy and better understanding of structural behavior have lead to the use of theories based on the ultimate and non-linear behavior of structures. Model work in late years has reflected these concepts. The problems of dynamic loads and the related dynamic response of structures, mentioned earlier, have added to the need for understanding the ultimate and non-linear behavior of structures.

In the past few years attention has been directed to this problem by the Defense Atomic Support Agency, and the Department of Civil Engineering of the Massachusetts Institute of Technology, under contract to DASA, has been studying the further development of the structural modeling technique. This project is an outgrowth of this development.

CHAPTER 2

SIMILITUDE

2.1 GENERAL

Similitude is the theory governing the relationships between the physical behavior of the model and that of the prototype. Through compliance with these relationships, the parameters chosen for the model, such as material properties and geometric scaling, fix the correspondence between model and prototype behavior.

As a result of the interaction of many forces, the correspondence between like phenomena at analogous points of the model and the prototype is most often selected as some constant. A more general view of similitude theory,^{(1) +} however, allows this correspondence to be a functional relationship. For example, we allow the relations of the form^(*) to hold for physical

$$\begin{aligned} (*) \quad \sigma_m &= f_\sigma(x, y, z, t) \sigma_p \\ M_m &= f_m(x, y, z, t) M_p \\ I_m &= f_I(x, y, z, t) I_p \end{aligned}$$

initial conditions and external influences (i.e., specified displacements and applied loads, and initial stress state). Here σ_m is the stress in the model at point (x, y, z) at time t and σ_p represents the stress state in the prototype at the corresponding point. M_m is the mass of the model at point (x, y, z) and I_m represents the moment of inertia of the model at the same point.

If all of these correspondence functions, f_σ , f_m , f_I , etc., were independent, then one could not readily transform model behavior into prototype behavior. Through the use of dimensional analysis, the interdependence of these functions can be determined as well as their relations to the basic fundamental quantities of length, time, mass, and if desired, temperature. Relationships will be obtained such as

$$t_m = \sqrt{\frac{f_u}{f_a}} t_p$$

+ Superscript numbers in parenthesis refer to references on page 61.

where t_m = time relative to the model
 t_p = time relative to the prototype
 f_u = correspondence function relating lengths
 f_a = correspondence function relating accelerations
or, in other words

$$f_t(x, y, z, t) = \sqrt{\frac{f_u(x, y, z, t)}{f_a(x, y, z, t)}}$$

This functional form of the similitude relationships opens broad possibilities in the modeling field. Although present techniques are not able to take full advantage of these possibilities, many new areas of engineering knowledge may be opened through their future development.

In almost all present day model work the correspondence functions are constants. These result from the selection of the model material and its inherent engineering properties as well as from other operational decisions. From a consideration of the pertinent physical dimensions related to the problem of the response of a structural model to air blast loading, the following similitude relationships result.

$$\lambda = \tau = z'$$

$$\mu = \rho = \rho'/z'$$

$$f_m(\epsilon_m) = f_p(\epsilon_m/z')$$

Where, according to the previous notation,

$$f_u(x, y, z, t) = \lambda = \frac{\text{length in model}}{\text{length in prototype}}$$

$$f_t(x, y, z, t) = \tau = \text{ratio of times}$$

$$f_\rho(x, y, z, t) = \rho = \text{ratio of stresses}$$

and

$$\mu = \text{ratio of densities} \left(\frac{\rho_m}{\rho_p} \right)$$

$$\rho = \text{ratio of moduli of elasticity} \left(\frac{E_m}{E_p} \right)$$

$$f_m(\epsilon_m) = \sigma'_m, \text{ the function relating stress and strain, a property of the material used.}$$

Since the same materials were used for the model as were used in the prototype, i.e., steel and "concrete", the gravity stresses were not scaled. This was not significant since gravity stress intensities were of small magnitude compared to over-all strength.

As explained later, the time scale was not equal to the length scale for the field test of the models. This resulted from practical limitations and the significance was investigated.

CHAPTER 3
PROCEDURE

3.1 PROTOTYPE

3.1.1 Prototype Selection. As a result of an earlier investigation carried out at M.I.T.⁽²⁾ several prototypes were selected for possible use as the basis for model studies. Several factors influenced the selection of the domes of Operation Plumbbob as the prototypes to be modeled. Some of these factors included ease of fabrication, limitations of laboratory fabrication, and subsequent shipment to the test site, ease of observing and evaluating the response of the model, and size of model test charge as compared with the various prototype weapon yields.

3.1.2 Prototype Dimensions. The prototype structures were spherical domes of 50 feet span diameter with a mid-surface curvature radius of 35.75 feet. This gives a height at the crown of 10.7 feet. The domes were 6 inches thick with two-directional reinforcing steel meshes placed near the top and bottom surfaces. The reinforcing consisted of 1/2 inch diameter reinforcing rods placed in great circular arcs with the maximum spacing distance equal to 6 inches. See Figure 3.1. The dome foundation consisted of a ring beam. The dome was joined to this so as to give a partially fixed support moment condition.

Prototype structures were tested at 20 psi, 35 psi, and 70 psi overpressure levels. As shown in Figures 3.2, 3.3, and 3.4, the prototypes failed at 35 and 70 psi while the one at 20 psi survived.

3.1.3 Material Properties. The dome was fabricated of normal reinforced concrete with deformed reinforcing rods of mild steel.

Tests by others⁽³⁾ on number four deformed bars showed variations in yield stress ranging from 39,000 psi to 52,000 psi, and ultimate stress variations from 67,000 psi to 85,000 psi. The prototype reinforcing would probably fall within these ranges also.

The concrete strength for the three domes are given in Fig. 3.5. Average values are given for seven-day strength and twenty-eight day strength. In addition, maximum and minimum values are given for the twenty-eight-day tests and for the cores tested eight days after the

domes were field tested. Curves have been drawn to represent the most probable strength versus age relationship for the concrete of each dome. On these, the probable strengths at the time of field testing are marked.

3.2 MODEL DOMES

3.2.1 Geometric Scaling. Since the model domes were small and demanded precise construction techniques, they were fabricated at M.I.T. and shipped to the test site. Each model dome was crated in a box that also served as a foundation during the test. To simplify the shipping and placement problems a model scale of $\lambda = 1/25$ was chosen. This gave model dimensions as follows.

base radius	24 inches
mid surface spherical radius	17.16 inches
height at crown	5.14 inches
shell thickness	0.24 inches

The scaling of the reinforcing resulted in 0.02 inch diameter wires at a maximum spacing of 0.24 inches.

3.2.2 Fabrication. Both the fabrication of the wire reinforcing meshes and the casting of the shells were done on wooden forms. These forms, which corresponded to the inside surface shape of the domes, were turned on a lathe. The forms used for the casting operation were fitted with a bushing at the crown point to permit the use of a scribe which was rotated around the dome.

The reinforcing wire, which came in a coiled bundle, was straightened before use in the fabrication of meshes by slightly yielding pieces of the desired length. Since a coating was placed on the wire by the manufacturer to prevent rusting, a bath in hydrochloric acid solution was necessary to remove the coating and prepare the wire for soldering.

The reinforcing wires were strung across the form in great circular arcs, radiating from pairs of four equally spaced poles located on the "equator" of the basic spherical surface. This mesh was then soldered at the crossing points in a regular pattern over the surface

and at all base edge points. The mesh thus formed held the correct shape during the casting operation. This is shown in Figures 3.6 and 3.7. A number of short wires were soldered to the meshes to serve as reinforcing chairs. Thus one mesh was positioned near the top surface and one near the bottom surface of the shell. Before casting, all reinforcing meshes were allowed to rust a moderate amount so as to increase their bond characteristics.

The model concrete consisted of a mortar mix of one part high early strength portland cement to four parts fine sieved sand and 0.7 parts water, i.e., (0.7:1.0:4.0). All comparisons or measurements of water, cement, and sand are based on weight.

The high sand to cement ratio was used in an attempt to maintain a Young's Modulus comparable to that of regular concrete. Because of the behavior of sand-cement mixes at these proportions, it was necessary to use an admix to obtain good workability. The additive used was Pozzolite Type A, made by the Master Builders Co. The quantity used was approximately 1.15 grams of admix per pound of cement.

The sand used in the mix was obtained from a standard concrete sand as defined in the ASTM standards. This sand consisted of particles ranging from .19 inch to less than .002 inches as shown in Figure 3.8. By passing the standard concrete sand through a No. 20 U. S. standard sieve and discarding the particles retained on the sieve a distribution as shown by the second curve of Figure 3.8 was obtained. Thus all particles of sand used in the microconcrete were not greater than .034 inches.

3.2.3 Casting. The forms were prepared for the casting of the domes by first applying a thin coating of paraffin wax and then an application of oil. Using this method the models separated from the spherical mold surface with relative ease.

In casting, as shown in Figure 3.9, the lower reinforcing mesh was held in place around the periphery and spaced above the form surface with wire chairs. The microconcrete was troweled under and over this mesh, being built up to the thickness where the top mesh was to be placed. The top mesh was then placed and peripheral masonite ring was clamped to the form base to secure the mesh in position. Wire chairs

gave the correct position over the dome. Again mortar was troweled over this and an excess thickness built up. This was then scribed off to the desired one-quarter inch thickness by a pre-set scribe which rotated from a bushing at the crown of the form. This set up is shown in Figure 3.10. The mortar was then allowed to set in a moist atmosphere for a day before being removed from the form.

The models were cured in a humid room for seven days. This room was maintained at a relative humidity of 95% at 75° F.

After curing, the dome was mounted on the plywood base by the casting of a base ring. This ring was firmly attached to the plywood base so as to secure the model against overturning due to the drag and rear side negative pressure created during the test. The base ring consisted of a 25-inch diameter hoop made of 1/4-inch diameter steel rod, which was cast inside a mortar of high strength. The dome reinforcing wires were anchored at their periphery by soldering to the steel hoop before casting the base. A cross-section of this base ring is shown in Figure 3.11.

3.2.4 Properties of the Model Materials. Tests on the reinforcing wire gave a yield stress of 65,600 psi and an ultimate stress of 82,800 psi for a strain rate of 0.00104 in./in./sec. At slightly faster strain rates ($\dot{\epsilon} = .00278$ in./in./sec.) the yield stress increased to 67,000 psi, and when slightly pre-yielded wires were tested yield stresses of 67,500 to 68,200 psi were obtained. A representative example of the stress-strain curves is shown in Figure 3.12.

These engineering properties seem reasonable for the model reinforcement when compared with the prototype steel properties. Although the yield stress is slightly high, the mechanism of failure in the dynamically loaded dome is predominantly a failure in the concrete and therefore this factor should not be critical.

The model concrete was tested as two-inch cubes. Table I gives the strengths for each of the three cubes tested for each model dome. Although a maximum strength of 4,800 psi and a minimum of 3,300 psi occurred, most models were within 10% of 4,000 psi mortar strength. Figure 3.13 shows various test data for this mortar mix. Each point

TABLE I

MICROCONCRETE STRENGTH

Specimen	f'_c	f'_c average	Age in Days
D1	4,200	4,308	43
	4,375		
	4,350		
D2	3,700	3,808	42
	3,875		
	3,850		
D3	4,350	4,321	41
	4,200		
	4,412		
D4	4,350	4,233	40
	4,150		
	4,200		
D5	4,188	4,096	39
	4,325		
	3,775		
D6	4,000	4,000	38
	4,125		
	3,875		
D7	4,350	3,858	36
	3,625		
	3,600		
D8	3,688	3,625	35
	3,562		
	3,625		
D9	4,450	4,800	34
	4,950		
	5,000		

(continued on next page)

TABLE I (Continued)
MICROCONCRETE STRENGTH

Specimen	f'_c	f'_c average	Age in Days
D10	4,212	4,096	34
	4,000		
	4,075		
D11	3,350	3,333	33
	3,450		
	3,200		
D12	4,325	4,283	32
	4,325		
	4,200		

is an average of three cube strengths, where each set is from a separate batch. Several cubes were instrumented with SR4-A-3 strain gauges to obtain the elastic modulus of this microconcrete. Two gauges were mounted on each cube such that the average axial compressive strain was measured. Results are shown in Figures 3.14, 3.15, and 3.16. In general the results agreed well with the often used relationship $E = 1000 f'_c$.

3.3 MODEL TESTING PROCEDURE

Since all of the models were to be tested in a surface mounted condition it was decided to mount the dome and its base on the inverted plywood cover. This was placed in a shallow hole such that the top of the base was flush with the ground surface. Prior to anchoring the base, the inverted plywood box cover was tamped full of soil to assist in preventing overturning. The plywood bases were bolted to the inverted covers as shown in Figure 3.17.

Model locations were as follows:

Expected Overpressure	Dome Number	Distance from GZ	Overpressure Probably Experienced (4)
20 psi	8	400 ft.	21.4 psi
	9		
30 psi	12	330	32.5
	7		
35 psi	11	310	37.5
	6		
40 psi	10	290	43.5
	5		
60 psi	3	250	61
	4		
70	4	230	74
	2		
80	1	220	82

This was obtained from Figures 3.18 and 3.19. (4)

3.4 CHARGE SCALING

As can be verified by checking the weapon of Operation Plumbbob, the geometric scaling factor of $1/25$, when applied to the prototype weapon according to the cube root law, does not give a model charge of 100 tons of TNT, as was used in this test. If the geometric scale was based upon the respective prototype and model test charges a λ of about $1/6$ would be required. This would have necessitated field construction of the models and probably fewer of them due to costs.

Having accepted the value of $\lambda = 1/25$, the positive duration time created by the model charge was too long for any corresponding model-prototype overpressure level. An initial investigation indicated that the deviation from true scaling was not significant. Therefore, the model study was continued with a reevaluation and more thorough inquiry to follow.

3.5 INSTRUMENTATION

Due to a number of factors such as cost, recording channels available, and the number of models being tested, it was decided not to instrument the models. Although various measurements were taken on the prototype domes, only deflections could have been measured on the models and compared with the prototypes.

This study was limited to an observation of failure pressure levels and failure mechanism, and a comparison with the prototypes.

The overpressure-distance data was acquired by the Ballistic Research Laboratories as part of other projects. This information was used to determine the actual test conditions for this project.

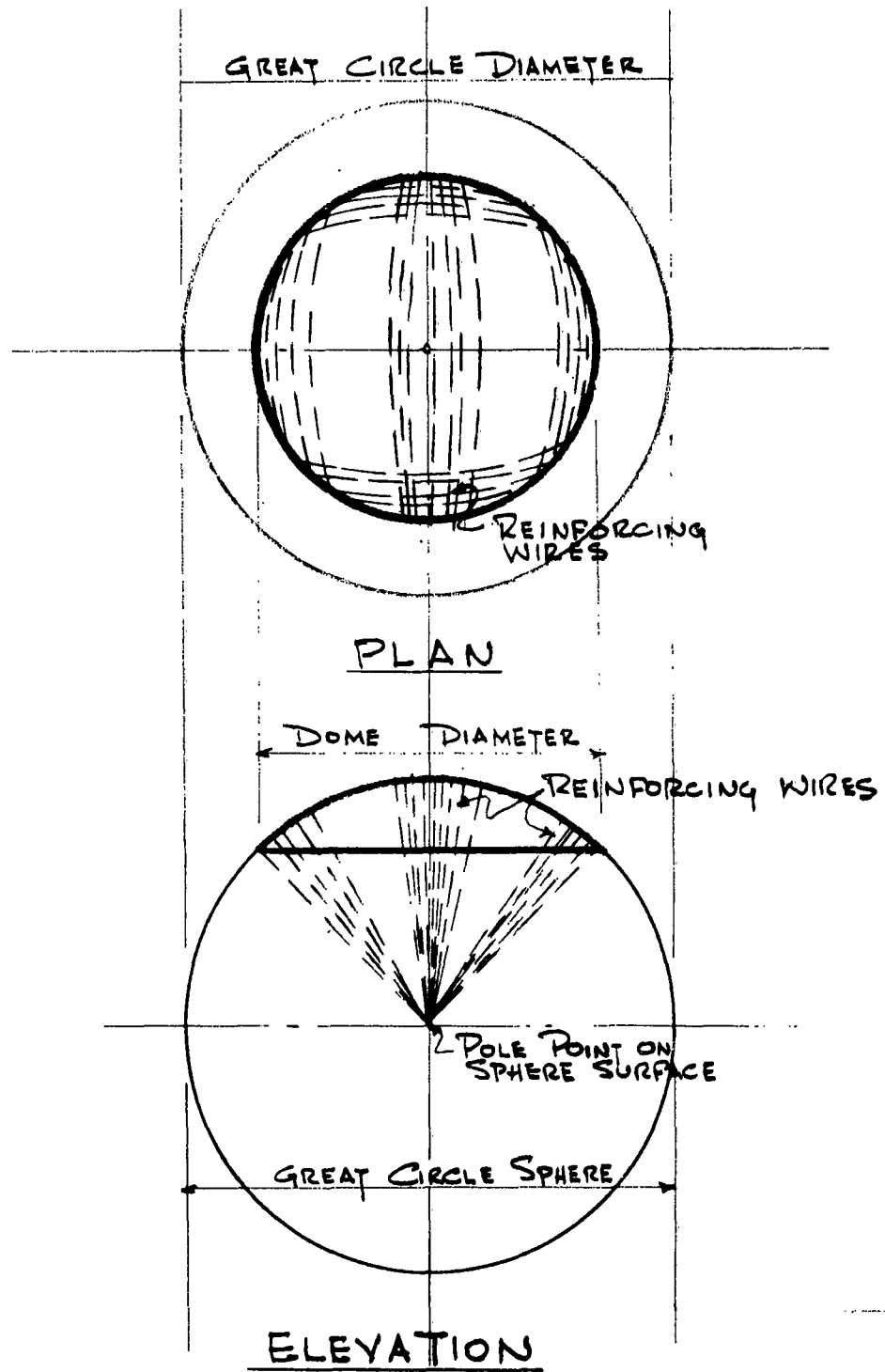


FIGURE 3.1 DOME REINFORCEMENT PLACING



Figure 3.2 Prototype Dome - 20 psi



Figure 3.3 Prototype Dome - 35 psi



Figure 3.4 Prototype Dome, 70 psi

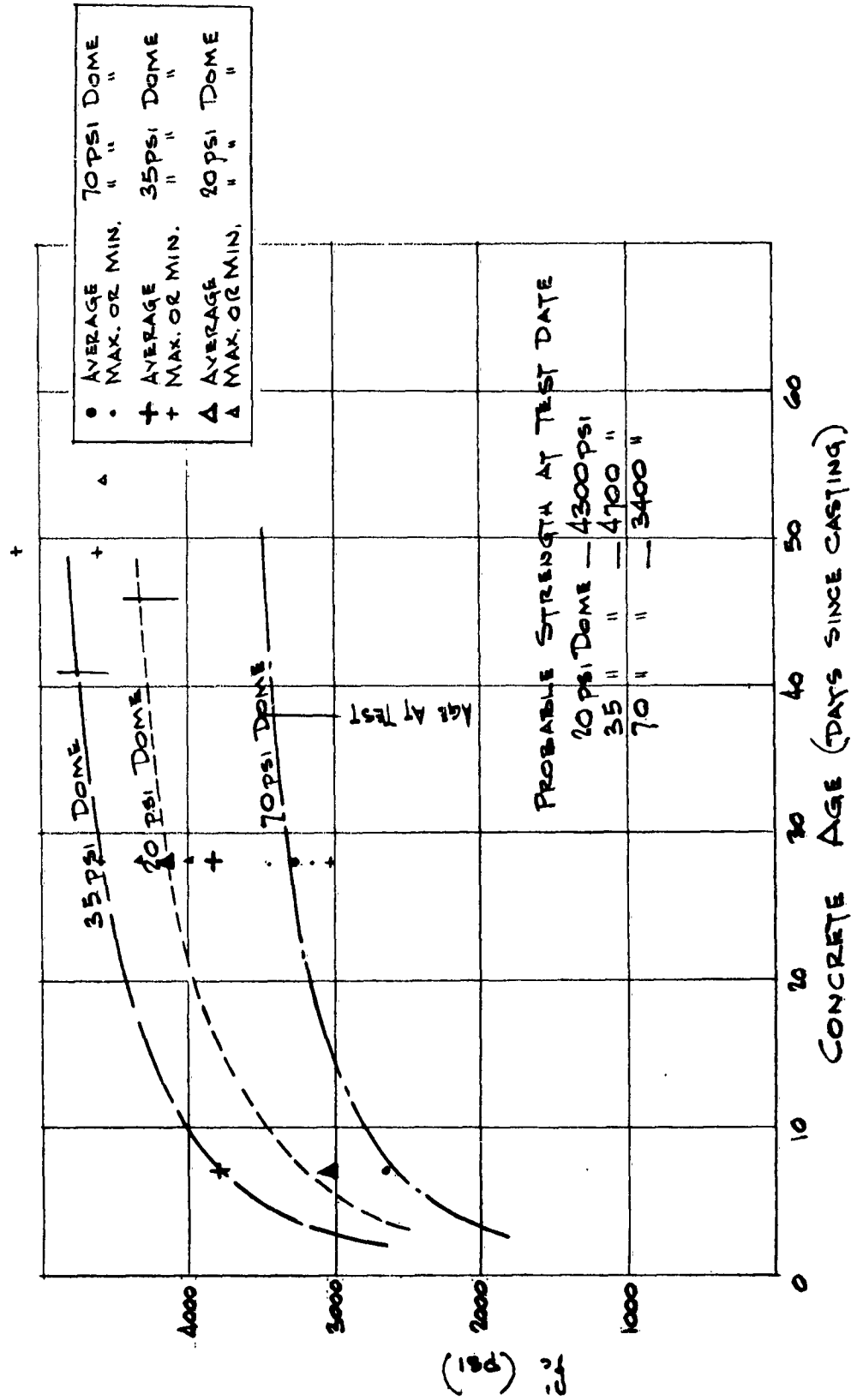


FIGURE 3.5 PROTOTYPE CONCRETE STRENGTHS



Figure 3.6 Mesh Fabrication

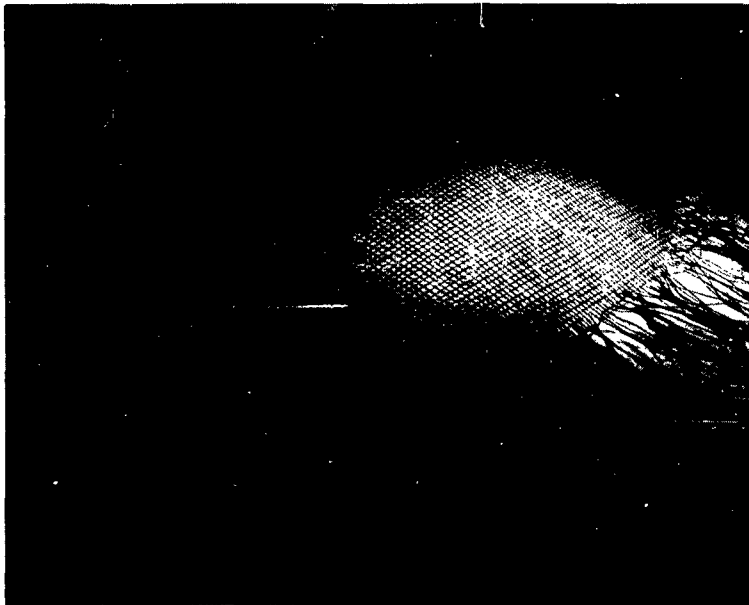


Figure 3.7 Reinforcing Mesh

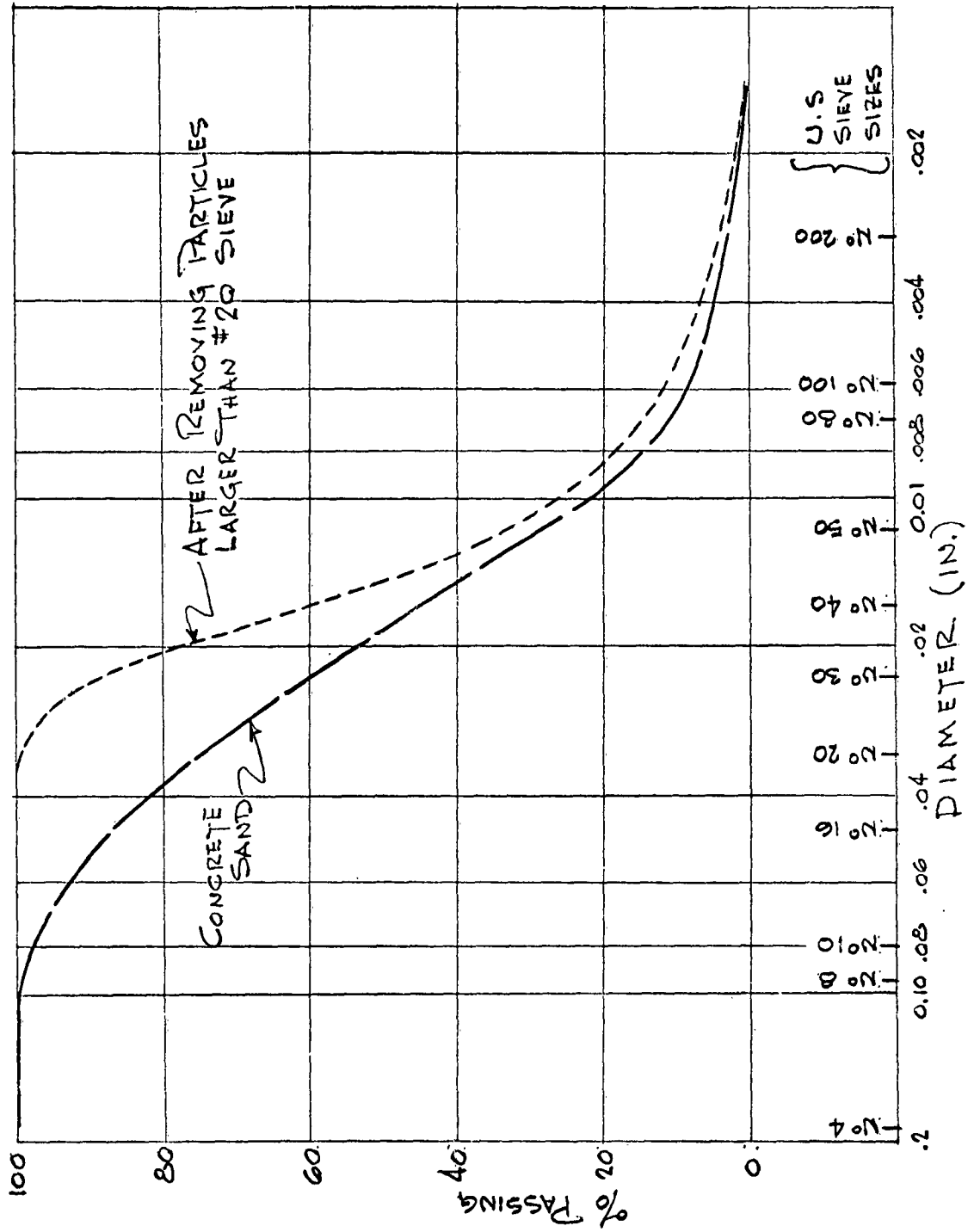


FIGURE 3.8 MODEL AGGREGATE SIZE DISTRIBUTION

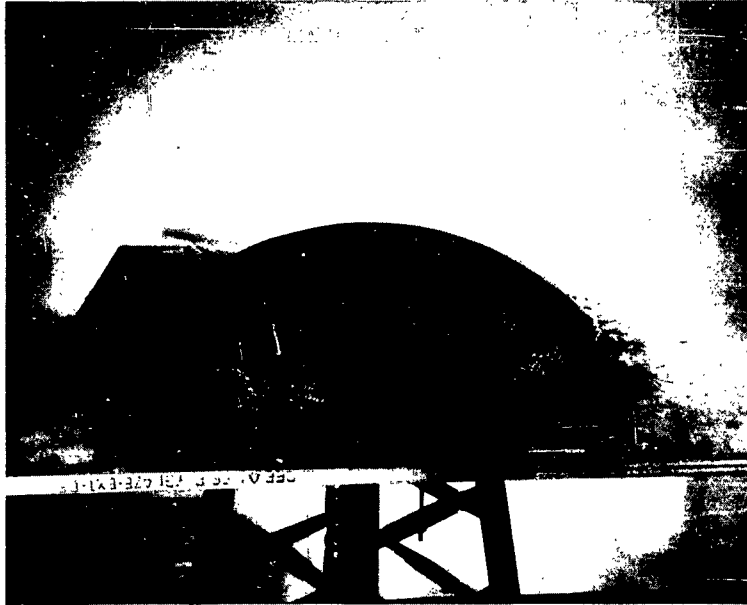


Figure 3.9 - Lower Mesh on Casting Form



Figure 3.10 Thickness Scriber

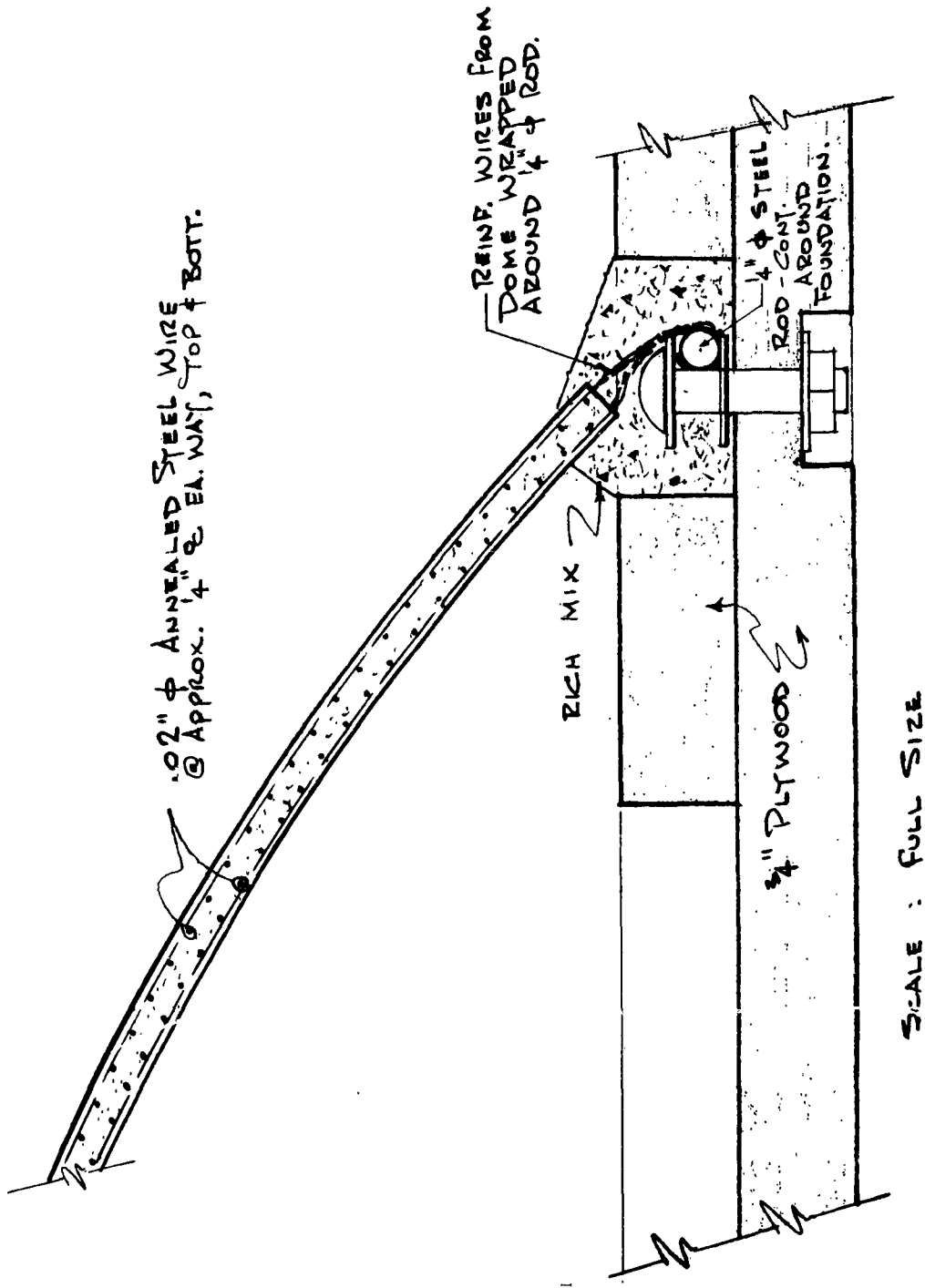


FIGURE 3.11 PART SECTION THROUGH DOME MODEL
SHOWING BASE RING

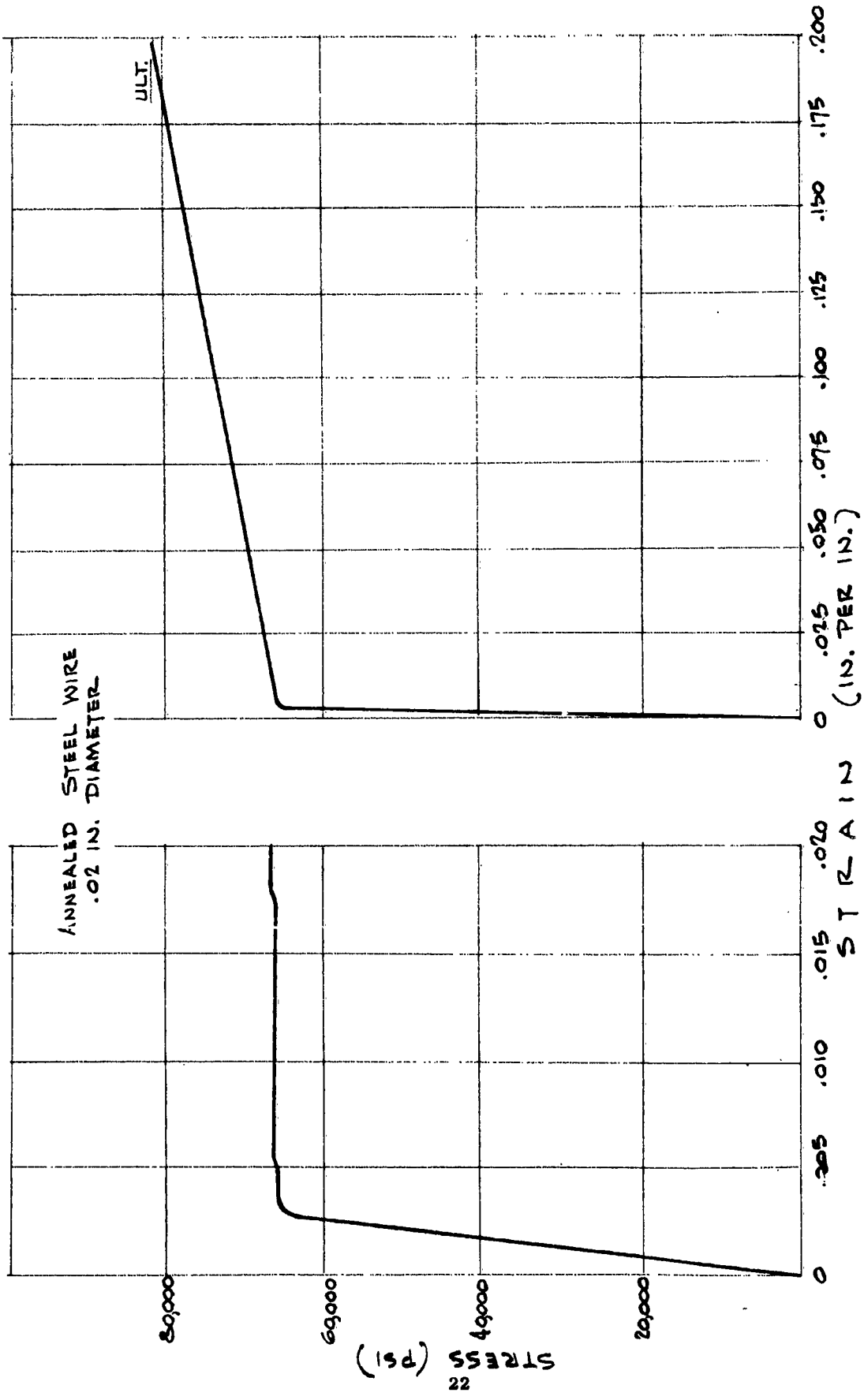


FIGURE 3.12 STRESS-STRAIN CURVE OF MODEL REINFORCING WIRE

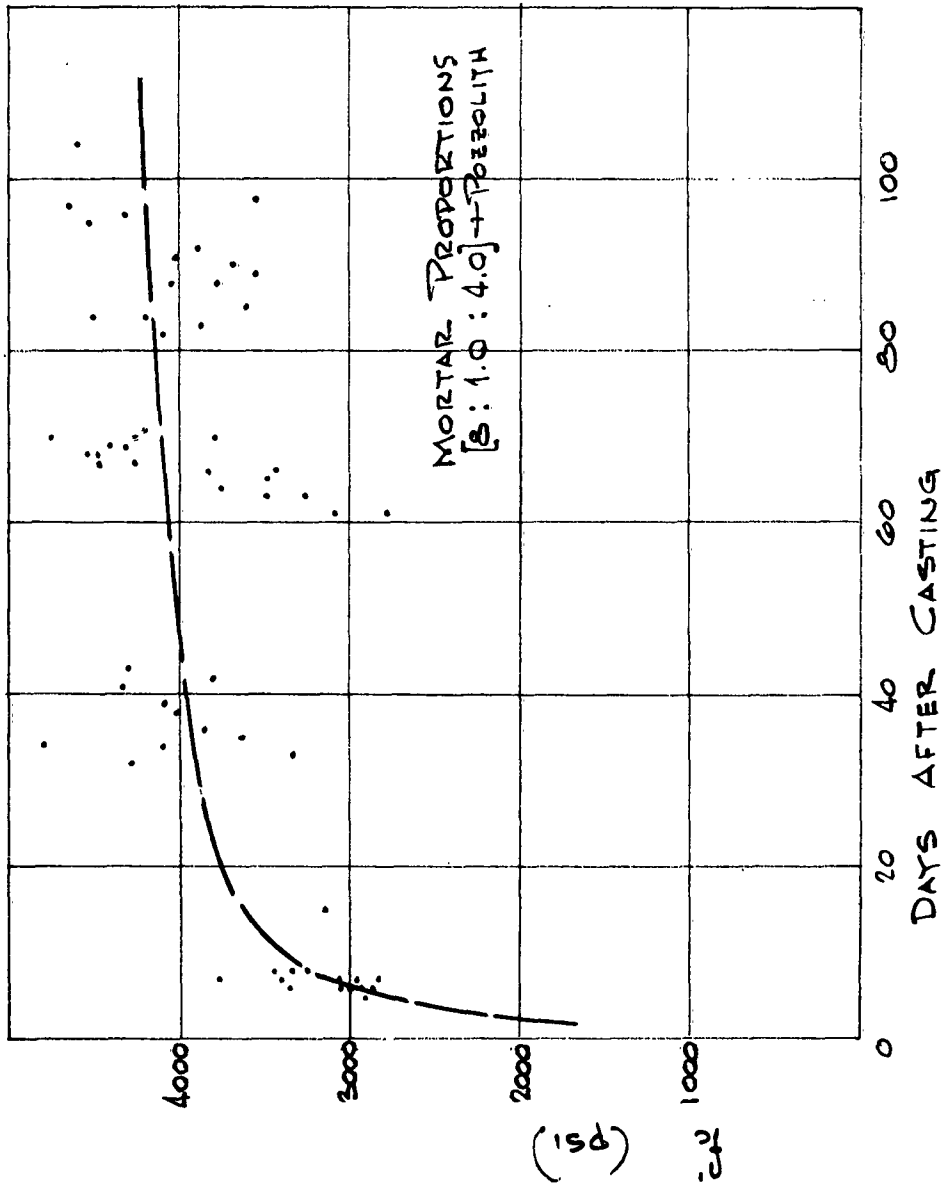


FIGURE 3.13 MORTAR STRENGTH vs. AGE

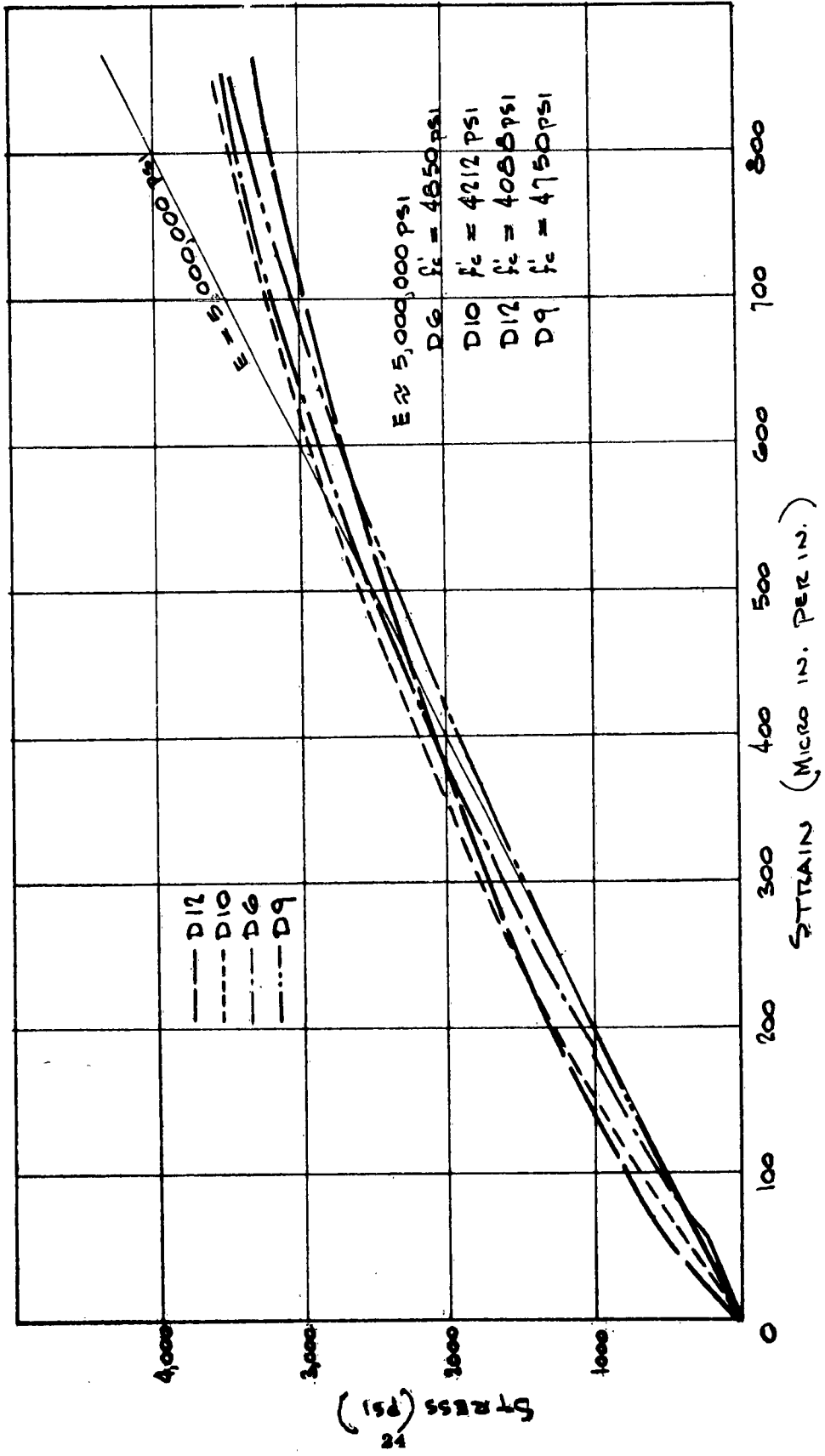


FIGURE 3.14 SOME MORTAR STRESS - STRAIN CURVES

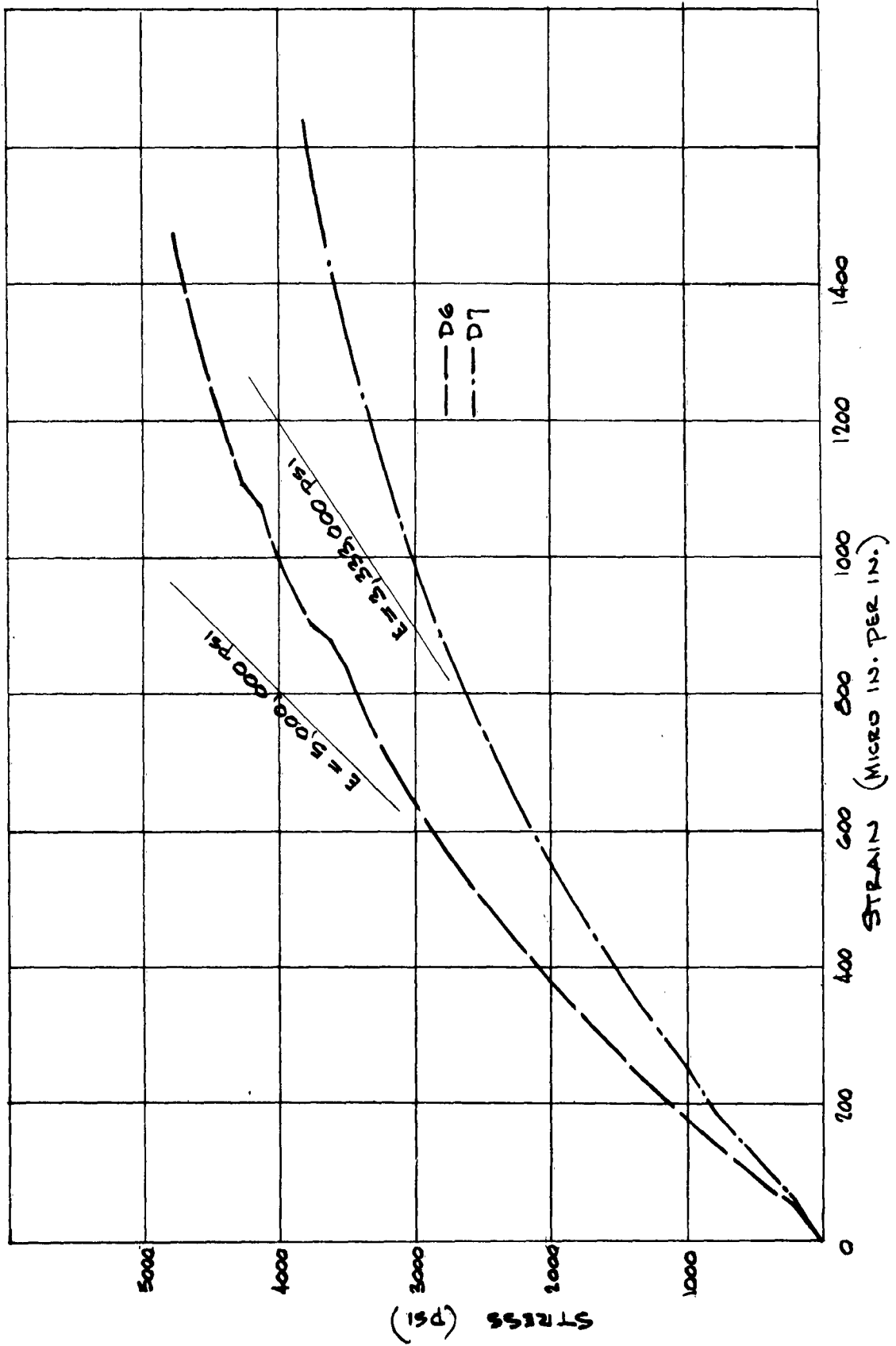


FIGURE 3.15 SOME MORTAR STRESS - STRAIN CURVES

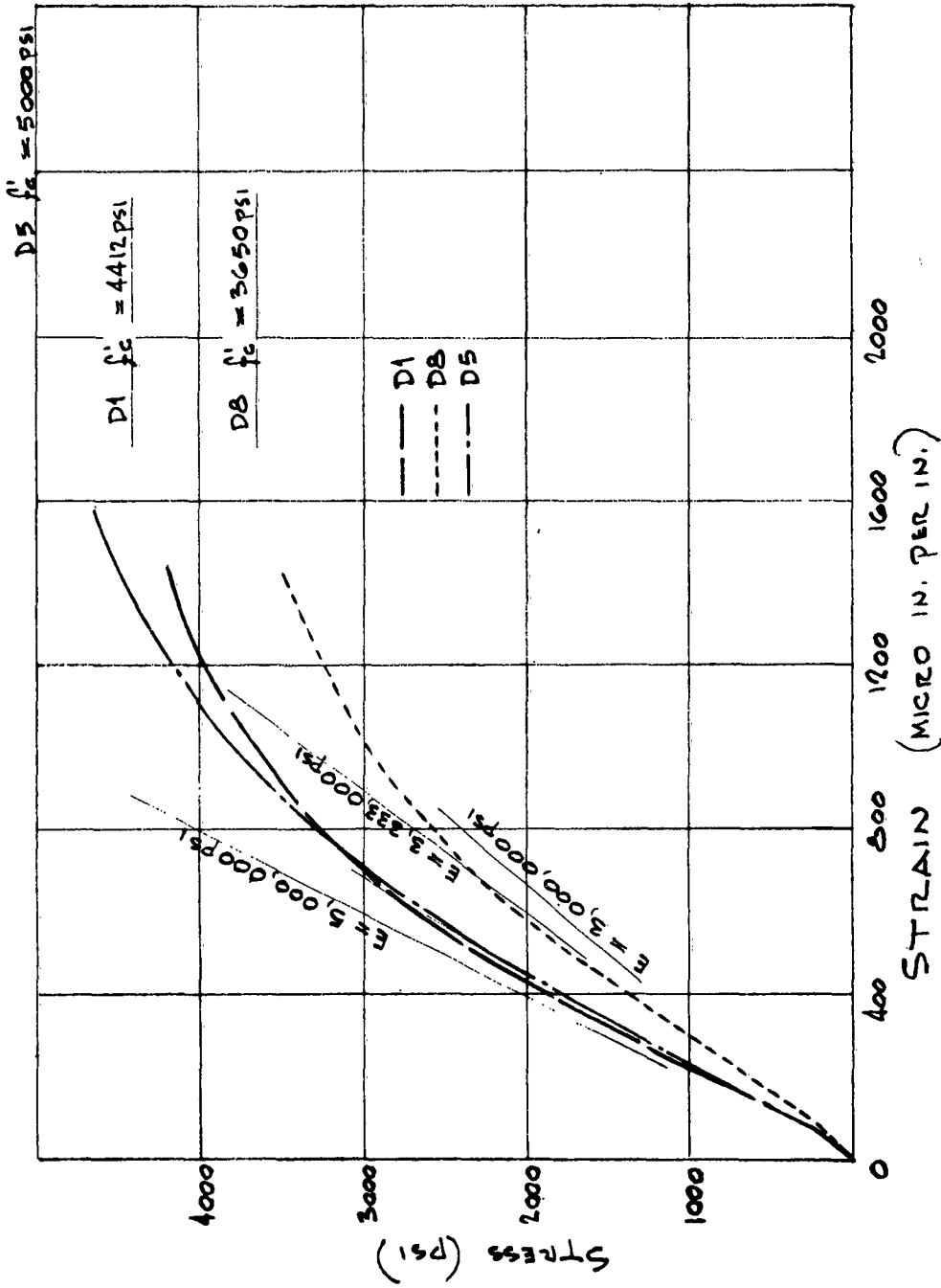
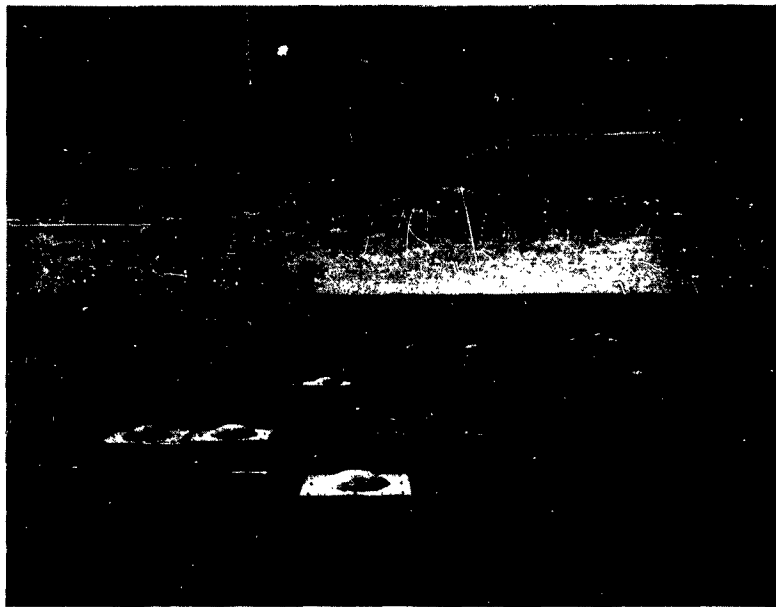


FIGURE 3.16 SOME MORTAR STRESS-STRAIN CURVES



**Figure 3.17 View of Model Installations Looking
Away from Ground Zero**

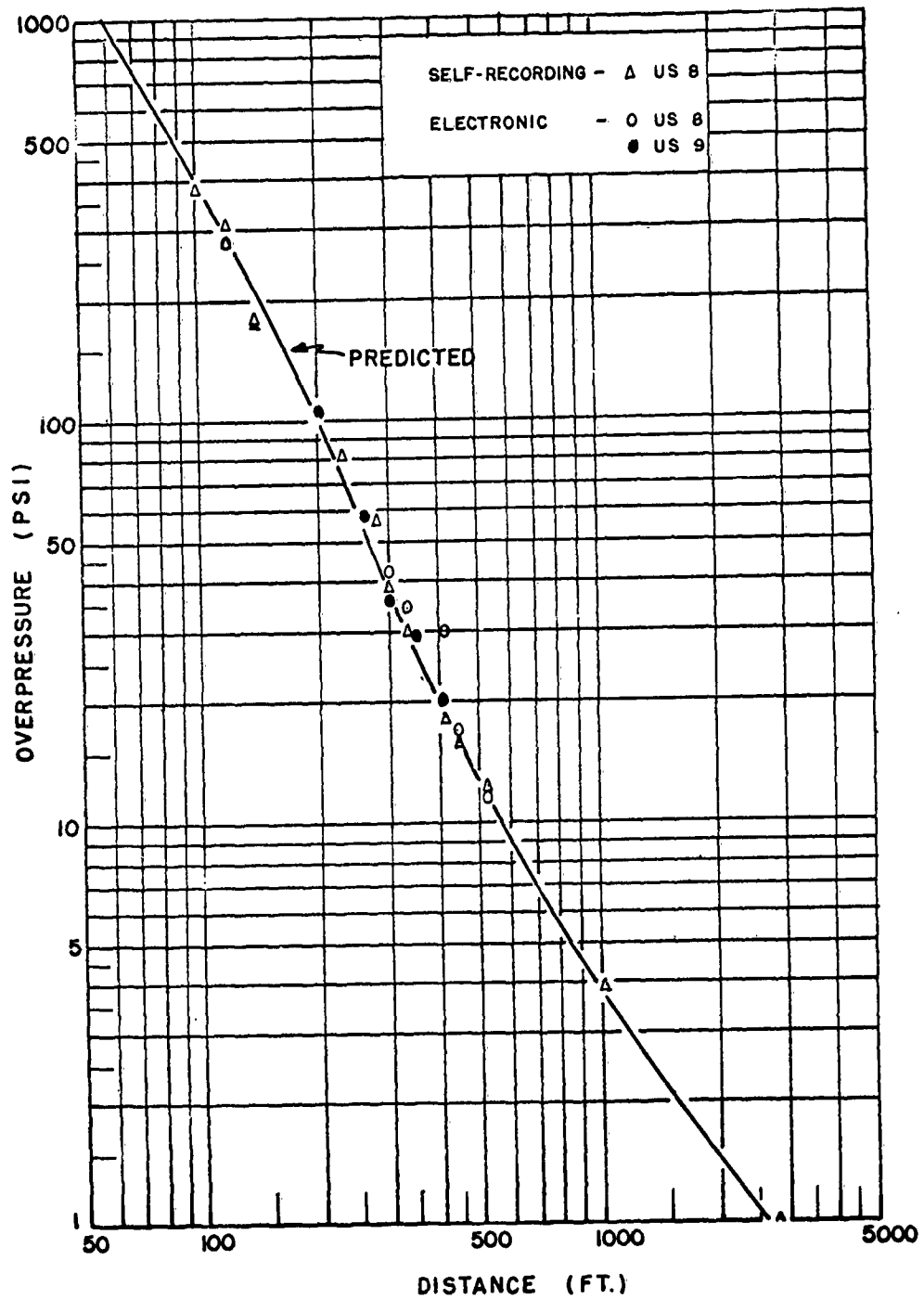


Figure 3.18 Predicted and Measured Overpressure versus Distance for a 100-Ton TNT Surface Burst

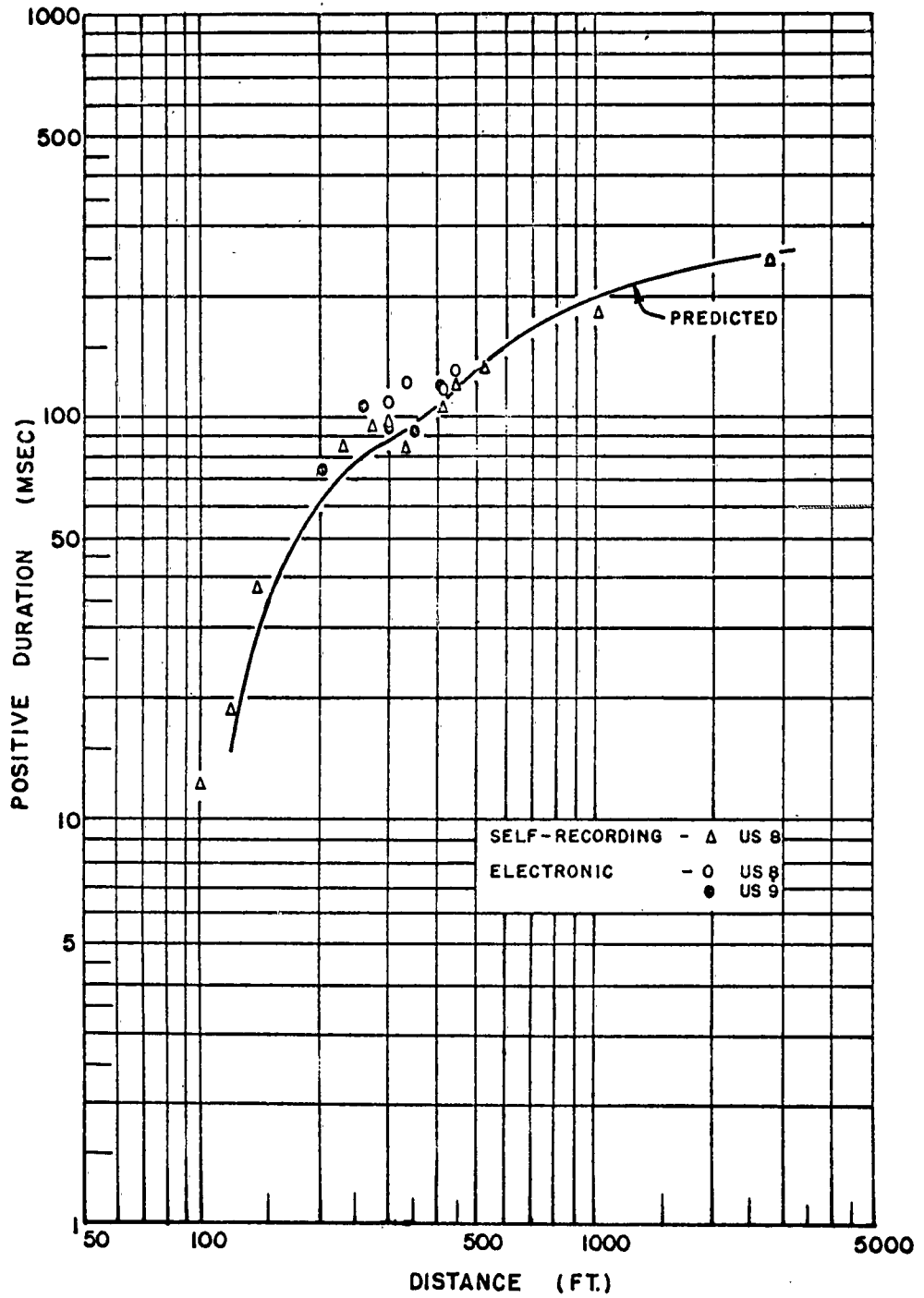


Figure 3.19 Predicted and Measured Positive Duration versus Distance for a 100-Ton TNT Surface Burst

CHAPTER 4

DYNAMIC TEST RESULTS

The layout of the model domes is shown in Figure 3.17. Model locations were staggered so that those closer to the charge would not interfere with the shock wave striking models farther out.

The before and after test appearances of the model domes are shown in Figures 4.1 through 4.17. Extensive damage occurred at the 80, 70 and 60 psi pressure locations. At the latter locations the models were stripped clean from the foundations leaving only portions of the reinforcing mesh. This behavior is due to the significant action of drag forces on the dome model immediately following the inception of failure.

Partial collapse occurred in the models at the 40 and 35 psi locations. Some missile damage was inflicted on the models at the 35 and 30 psi locations. These missiles were large chunks of soil which were thrown out from the charge crater. This type of action usually accompanies a high explosive detonation in the type of soil found at the Suffield test site.

Good comparisons of the failure mode can be made from the models of Figures 4.2, 4.8 and 4.10, and the two prototypes of Figures 3.3 and 3.4.

The difference between the predicted overpressure - distance relationship and those actually measured in the field are shown in Figure 3.18. The related positive duration curve is shown in Figure 3.19.⁽⁴⁾ The measured values show good agreement with the predicted values. A uniformly, i.e., spherical, expanding blast wave was indicated. The predicted values are therefore used in identifying the test conditions.



Figure 4.1 80 psi Dome PreShot



Figure 4.2 80 psi Dome PostShot

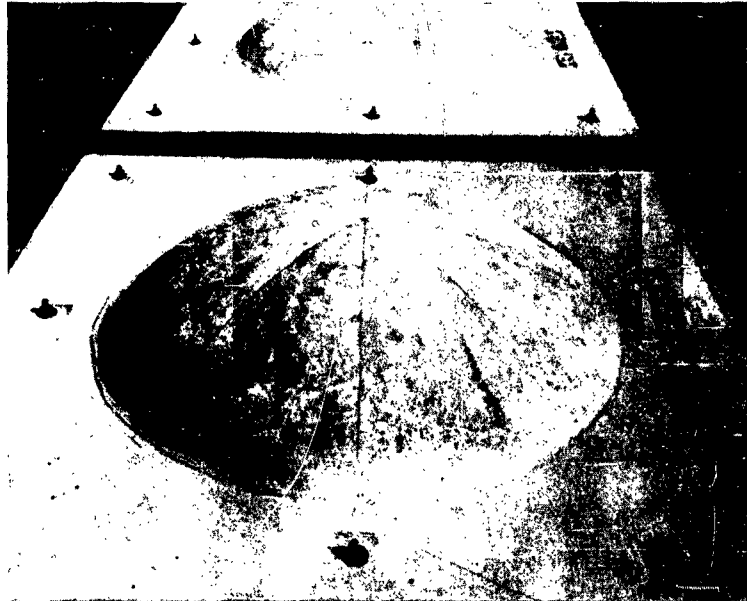


Figure 4.3 70 psi Domes PreShot

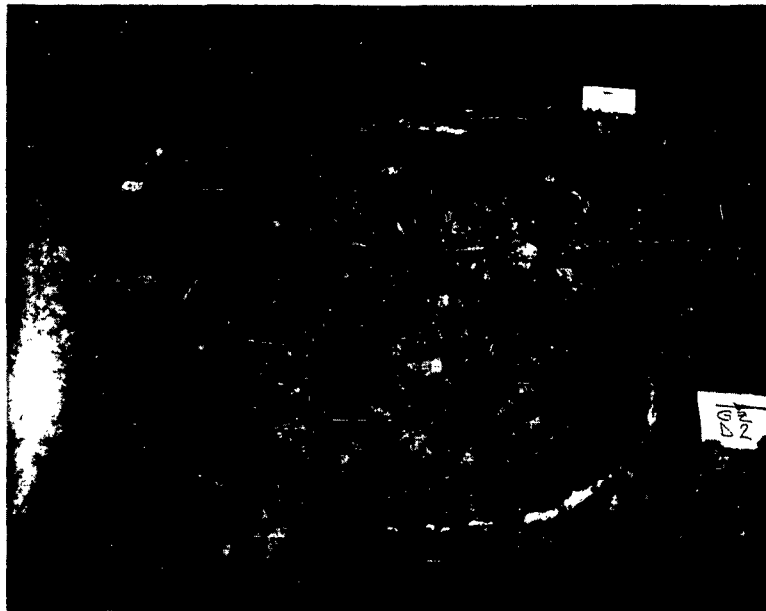


Figure 4.4 70 psi Domes Postshot



Figure 4.5 60 psi Dome Preshot

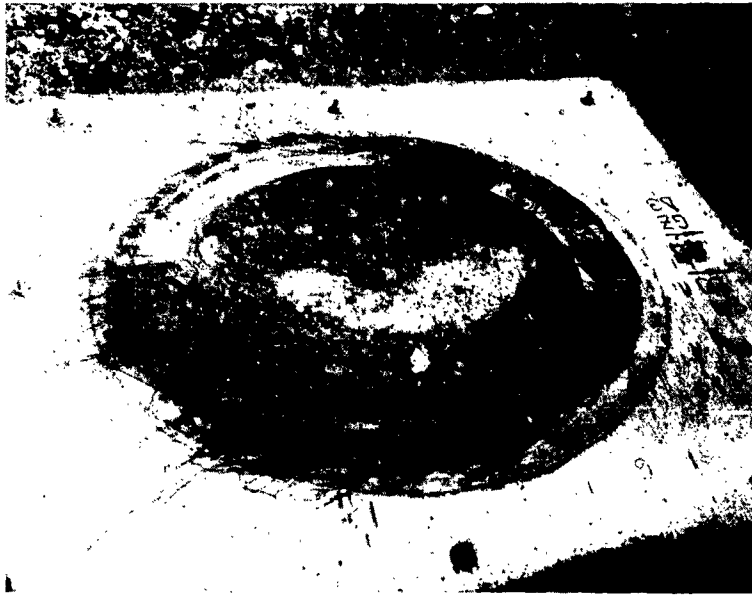


Figure 4.6 60 psi Dome Postshot

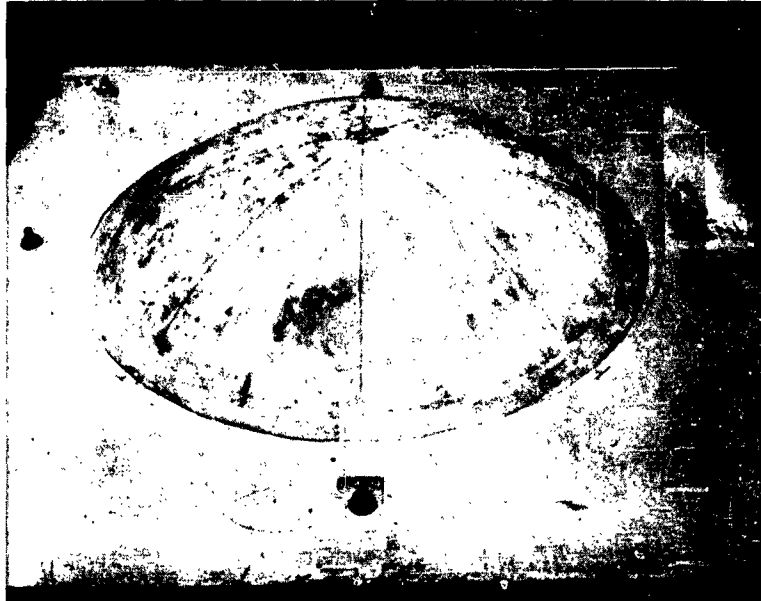


Figure 4.7 40 psi Dome Preshot



Figure 4.8 40 psi Dome Postshot



Figure 4.9 40 psi Dome Preshot

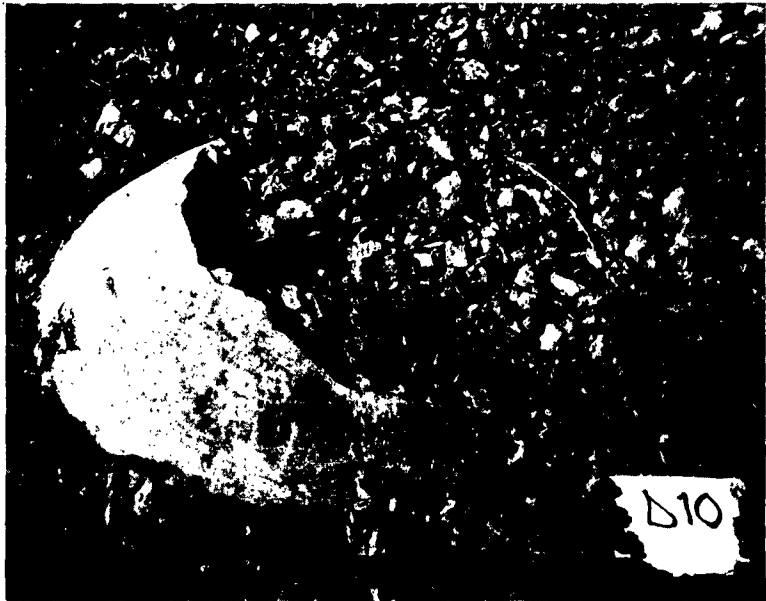


Figure 4.10 40 psi Dome Postshot



Figure 4.11 40 psi Dome Preshot

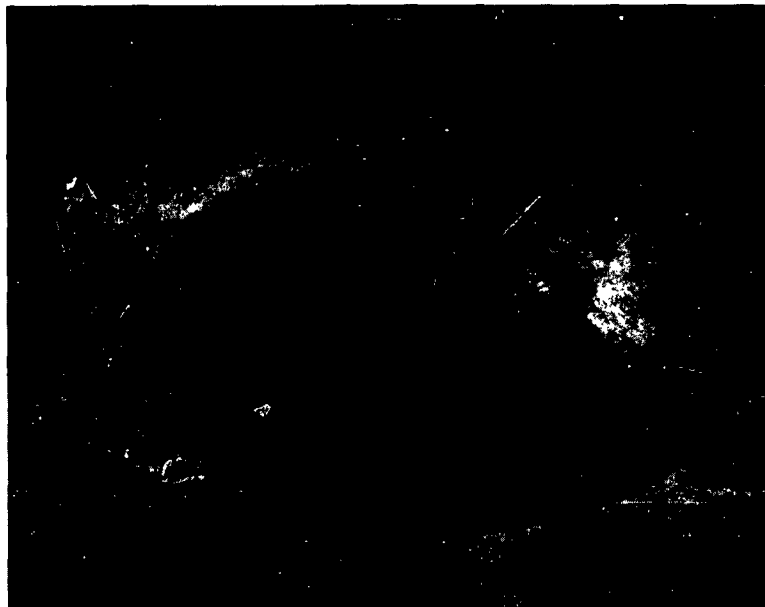


Figure 4.12 35 psi Dome Postshot (note missile damage)

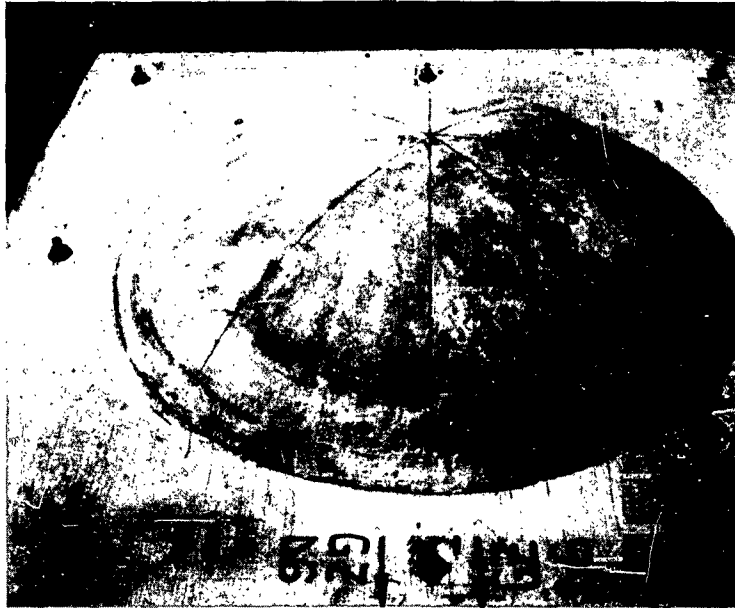


Figure 4.13 35 psi Dome Preshot



Figure 4.14 35 psi Dome Postshot

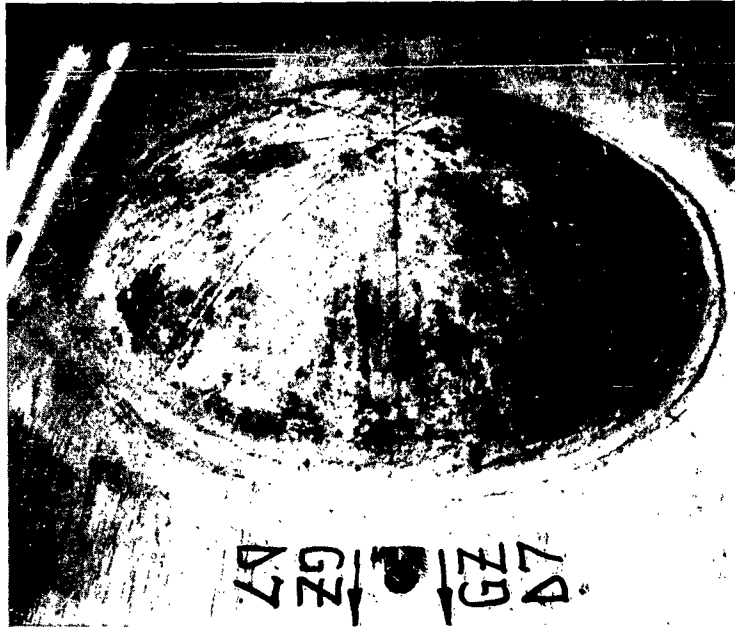


Figure 4.15 30 psi Dome Preshot

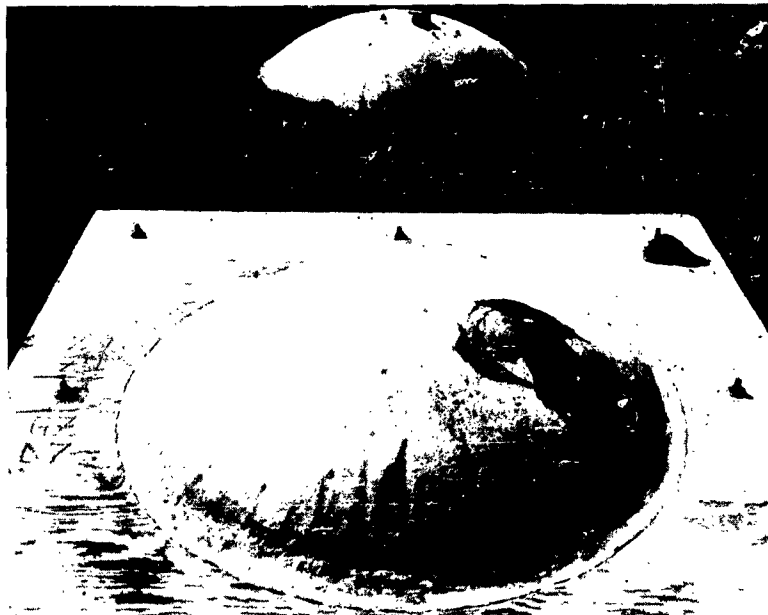


Figure 4.16 30 psi Dome Postshot

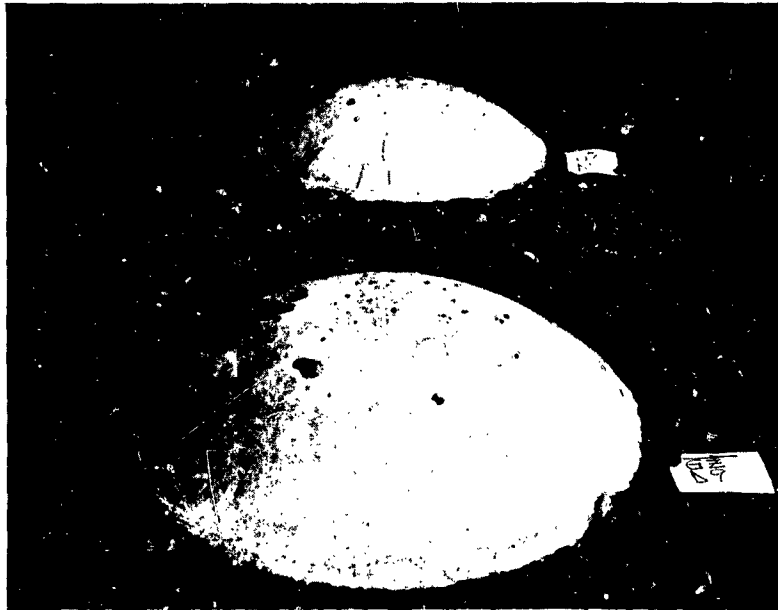


Figure 4.17 20 psi Dome Postshot

CHAPTER 5

SIGNIFICANCE OF DURATION TIME SCALING

5.1 INTRODUCTION

The scaling used in the construction of the model required that the following similitude relations be satisfied:

- (1) Length of model = $\frac{1}{25}$ x length of prototype
- (2) Pressure on model = pressure on prototype
- (3) Time on model = $\frac{1}{25}$ x time on prototype

In the field tests of the models it was not possible to satisfy the third similitude requirement, and it is therefore necessary to determine if violation of this relation substantially affected failure levels of the models.

5.2 PROCEDURE

5.2.1 General. No comprehensive analytical method is available that includes all the effects which are of importance in the prediction of collapse of a dome subjected to a shock loading. However to estimate the magnitude of the error introduced by not correctly scaling the duration time of the load, a simplified design approach can be used.

Methods have been suggested^(5,6,7) that introduce the following simplifications:

- (1) An "average" type load-time relation is used.
- (2) The dynamic response is approximated by a one degree of freedom analysis.
- (3) The membrane theory is used to determine the stresses in the dome.

Reference^(6, pg. 34) states the conditions under which the membrane theory may be used as a valid approximation.

5.2.2 Load: The method used to determine the load is that suggested in Reference⁽⁵⁾. In this method a number of points are chosen to cover the surface of the dome. The time of arrival of the blast wave and also its angle of incidence are different for each point. Therefore a different pressure vs. time curve is obtained for each point. In computing the

reflection and drag coefficients for domes, those given in Ref. (7) were used because they are the most recent.

Having the pressure-time curves for individual points on the dome, the average pressure for the leeward and windward sides was calculated by a simple arithmetic average of the appropriate points taken at each time interval. The leeward and windward pressures are then separated into symmetric and anti-symmetric components. By repeating the above calculations for a succession of time intervals an average symmetric and anti-symmetric pressure-time curve can be developed following the method of Ref. (5). Since these lengthy computations were to be repeated for a number of different models and prototypes at differing pressure levels a short digital computer program was written which performed the above computations.

5.2.3 Dynamic Response. After having obtained the variation of the average symmetric and anti-symmetric pressures with time, the dome is then considered as a one-degree of freedom system vibrating at the circular membrane frequency. In theory, this frequency is a function of the elastic moduli of the dome material, which would differ slightly for each model and for each prototype. An average value of the frequency for all models was obtained by applying the scaling laws to the experimental frequency of the prototype field tests⁽¹⁰⁾. For the range of the parameters of interest the pressure response is insensitive to small differences in the frequency. Since it is only desired to compare the effect of duration time, it was not considered necessary to conduct tests for the determination of the model frequencies.

The acceleration pulse extrapolation method was used to integrate the dynamic equation of the one-degree of freedom system⁽⁸⁾. The computations were carried to the first maximum value of the pressure-time curve.

5.2.4 Capacity. The final task was to relate the peak dynamic symmetric and anti-symmetric pressure to the capacity of the dome structure. The capacity of a reinforced concrete dome under uniform compressive radial load (membrane theory) can be computed from equation(1)⁽⁹⁾.

$$(1) \quad r_c = (0.85 f'_{DC} + 0.9 p f_{Dy}) \frac{2t}{r}$$

where r_c = capacity of dome under uniform radial load
 f'_{DC} = the dynamic strength of the concrete in axial
 compression
 p = steel ratio
 F_{Dy} = the dynamic yield strength of the reinforcing steel
 t = dome thickness
 r = radius of dome

For a dome it can be easily visualized that the anti-symmetric component of the pressure is a more severe loading condition. That this is the case can be explained qualitatively by postulating that the symmetric radial pressure is carried by the entire dome while the anti-symmetric pressure is carried by a series of arches parallel to the wave front. This would indicate that the effect of the anti-symmetric load should be weighted approximately by a factor of two. Ref.⁽¹⁰⁾ places the above argument on a quantitative basis.

If we define the required capacity (C) by the relation

$$(2) \quad C = P_{sym} + k P_{anti-sym}$$

where k is the factor mentioned above and the P 's refer to respective pressure responses, then the final computation would be to compare C to the dome capacity (r_c) from equation (1). If C is greater than the actual capacity, failure of the dome is indicated, while if C is less than r_c then survival is predicted.

To illustrate the effects of not satisfying the similitude relations for the duration times, the required capacity will be computed at various pressure levels:

- A) for the duration time actually measured in the field test. (Designated by C_F)
- B) for the duration necessary to satisfy similitude. (Designated by C_S)

Since the duration time is a parameter of the loading, it should be noted that comparison of the required capacities does not involve any assumptions regarding material properties or dynamic strength increases.

5.3 RESULTS

Figures 5.1 shows these curves for models in the 43 psi and 37 psi overpressure regions. These models were chosen for illustration because they bracket failure, namely the model at 37 psi survived in the field test, while the model at 43 psi failed.

The pertinent strength data for these models are summarized in Table A.

TABLE A

P_{so}	f'_c *	Approx. Strain Rate in./in./sec.	$\frac{f'_{DC}}{f'_c}$ **	f'_{DC}
43 psi	4096 psi	.7	1.3	5325 psi
37 psi	3333 psi	.6	1.3	4333 psi

* results of cube tests

** Norris, et. al., Chapter 4 (Ref.8)

For both models:

$$\begin{aligned}
 t &= 0.25 \text{ in.} \\
 r &= 17.16 \text{ in.} \\
 f_{Dy} &= 42,000 \text{ psi} \\
 p &= 0.011
 \end{aligned}$$

Substitution of the above values in equation (1), permits the computation of the capacity for each model:

P_{so}	$r_c =$ Capacity (psi)	Result of Field Test
43 psi	139	Failed
37 psi	115	Survived

For the model in the 37 psi region, Figure 5.1, the actual capacity is indicated by the heavy horizontal line. The dashed curve represents the

required capacity for durations measured in the field, (C_F), while the solid curve represents the same quantity for the durations necessary to satisfy similitude, (C_S). The cross-hatched portion of the diagram indicates the region for which the capacity exceeds the predicted required capacity and therefore the region of survival. For a given capacity (vertical axis) the difference in horizontal intercepts of the dashed and solid curves (such as c-d) is a measure of the difference in overpressure failure levels caused by inability to satisfy similitude. It can be seen that this is an exceedingly small difference (less than .3 psi) and also that the longer duration experienced in the field slightly decreases the overpressure at which failure occurs. Alternatively, this may be thought of as a slight increase in the load sensed by the model at a given overpressure. Point A indicates the conditions that prevailed in the field for the model and predicts correctly that the model survived.

The above remarks also apply to point B in Figure 5.1 for the model at the 43 psi overpressure level. Here, however, point B, which describes the model strength and overpressure level in the test, lies in the failure region and again correctly predicts the results of the field test.

5.4 EFFECT OF DURATION TIME

Based on the preceding results, failure to satisfy the similitude requirement with respect to duration causes a slight decrease in the overpressure at which a given model would fail. The actual value of the decrease, in this case about .3 psi, is not meaningful since it is based on a one-degree of freedom, membrane analysis. However, this analysis does reflect the gross features of the behavior of a dome to shock loading, and it can be reasonably assumed that a more complete analysis, were it available, would also show that the error is insignificant.

As a further understanding of the conditions for which the similitude requirements of duration can be safely violated, consider Figure 5.2 which is the predicted pressure-time variation for a point on the dome. The time ordinate, which is drawn to scale, shows that the actual duration is approximately four times that necessary for similitude.

For a one-degree of freedom elastic system, it can be demonstrated Ref. (8) that if the duration of the load is large, the time for peak

response is less than the natural period. The natural period of the models is indicated on the figure, and it can be seen that for times less than the natural period, there is only a minor difference in the pressure ordinates. By virtue of the similitude relations, the natural period of the model will be a relatively small quantity and the error introduced by violation of duration similitude can be ignored in general.

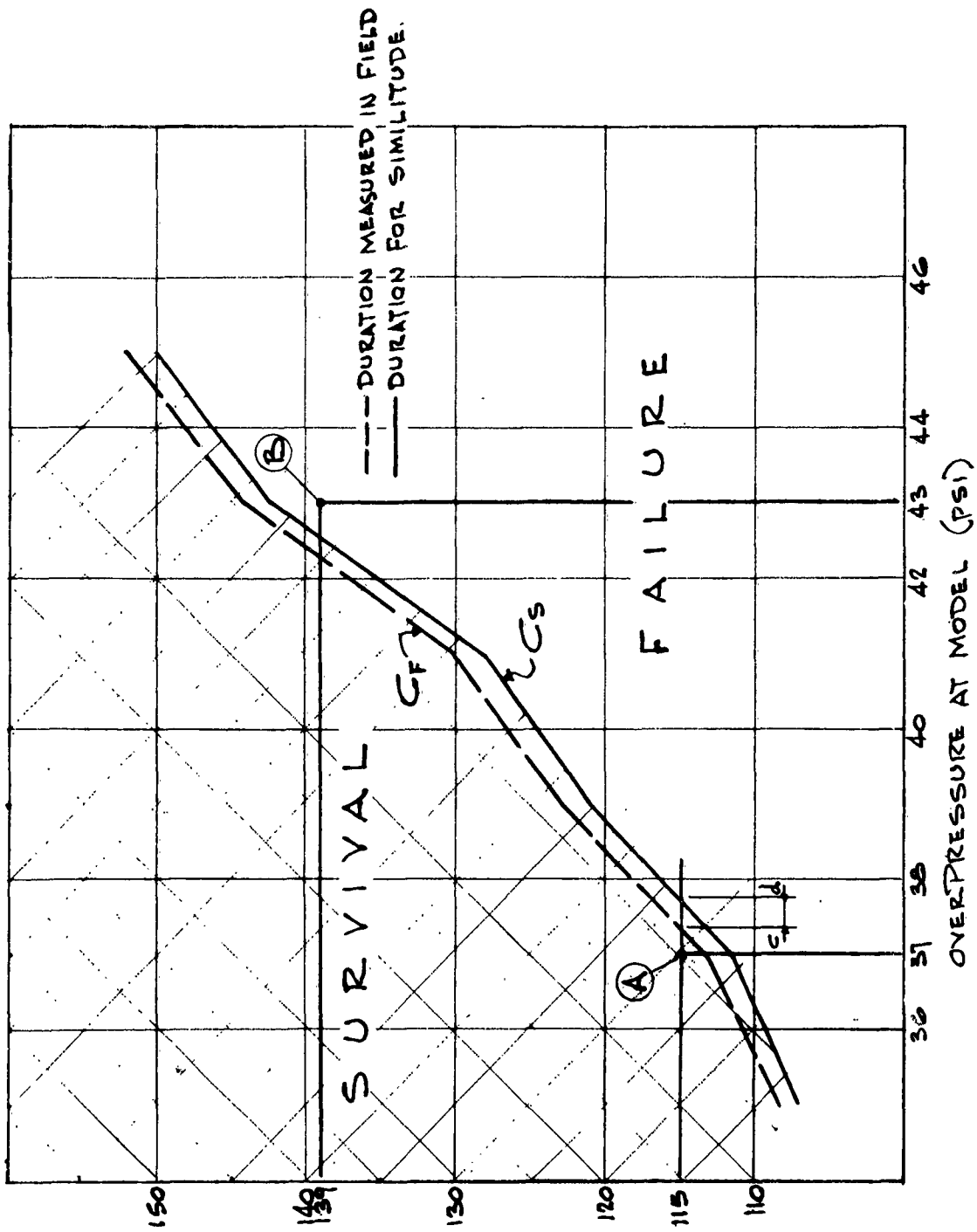


FIGURE 5.1 EFFECTS OF DURATION TIME ON MODEL BEHAVIOR

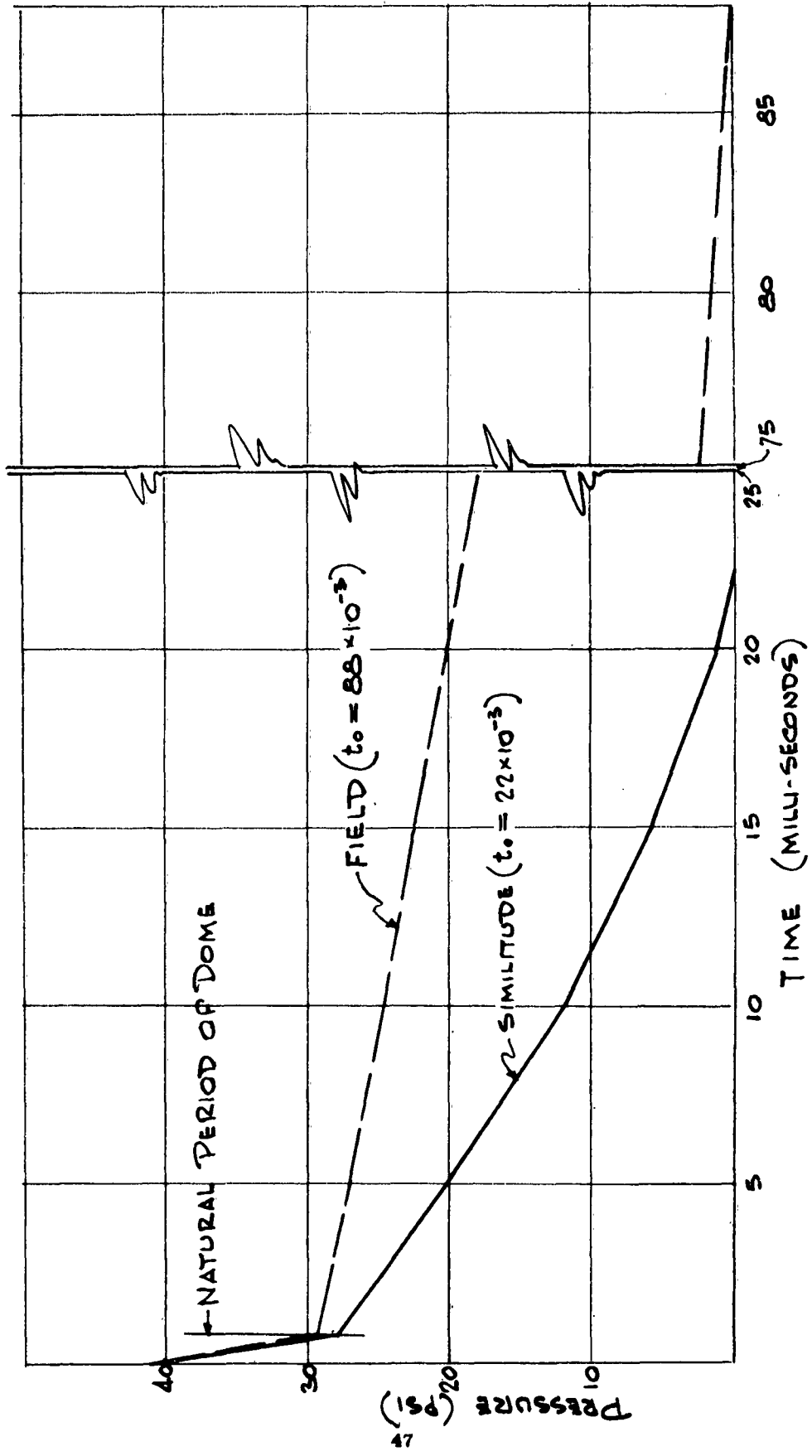


FIGURE 5.2 PRESSURE-TIME CURVE FOR TYPICAL POINT ON MODEL

CHAPTER 6

STATIC TESTS ON MODEL DOME STRUCTURES

6.1 INTRODUCTION

The purpose of these tests were to determine the static strength of the model concrete domes used in the Canadian High Explosive test of August 1961.

6.2 LOADING PATTERN

A uniformly distributed radial load on the models was approximated by 48 discrete loads. The surface of the dome model was divided into 16 equal areas and each of these was then subdivided into three equal areas as shown in Figure 6.1. It was decided to use an equal area method of distribution since the actual location of the load points on the model could then be easily determined and marked. Also it would yield a regular pattern of discrete load points for the loading apparatus. It was decided that if fairly large pads were used to distribute the load at each point, a good approximation to a uniform load would be obtained with 48 loads. It was felt that the tendency of the discrete loads to punch through the shell and the bending in the shell between load points would not be significant in this size model.

6.3 LOADING SYSTEM

Sixteen hydraulic jacks, manufactured by Hannifin Company (model CBB-HL21C) were used to load the models. These jacks had a 2 inch bore, 4 inch stroke and 2000 psi normal working pressure. The load from each jack was applied to the model through a hi-strength (7075-T6) aluminum extension. Each jack extension transmitted the jack force to a triangular steel plate which spread the load into three equal loads. Figure 6.2 is a drawing of the load-spreading device and Figure 6.3 is a photograph of the assembled loading system using all small pads.

6.4 LOADING FRAME

A test frame constructed of rolled structural steel sections with bolted connections was designed and fabricated to contain the

model and the loading system. A drawing of the test frame is shown in Figure 6.4. In order to determine the exact line of action of each hydraulic jack and the location of its intersection with the top of the frame, the area loaded by each jack was divided into three equal sub-areas. First, the center of gravity of each sub-area was calculated and then the location of the center of gravity of the triangle formed by these three points was determined. This gave the radial line of action of the respective jacks. The jacks were attached to 4 inch tee sections welded to the test frame. The locations of the connection points were found by placing a theodolite at the spherical center of a model dome when positioned in the test frame, and sighting the radial angles corresponding to the calculated jack axis. Figures 6.4 and 6.5 show the assembly.

6.5 INSTRUMENTATION

The applied loads were measured by 8 load cells built into the jack extensions. These load cells were distributed on the model as shown in Figure 6.1. An interior portion of each extension used as a load cell was reamed out for a length of 4 inches leaving a wall thickness of $\frac{3}{32}$ inch. Eight C-7 strain gauges were mounted on the outside of this hollow rod as shown in Figure 6.2 (4 were active gauges and 4 were dummy gauges). These gauges were connected into a Wheatstone bridge circuit and the signal recorded on an 18 channel Consolidated Electrodynamics Corporation oscillograph unit.

Each load cell was calibrated on a 10,000 pound capacity, Rielle Brothers, beam testing machine, in increments of 500 pounds up to a maximum load of 7000 pounds.

6.6 TEST PROCEDURE

Each load point was located on the dome model surface. The model with its plywood base was then positioned in the test frame and bolted through the base to the lower beams. The loading pads and triangular spreaders were placed on the model and the jack extensions were manually pulled out to rest on the spreaders.

As standard procedure, a "zero" load point on the CEC record was noted at this time and then the pressure in the loading system was raised

to approximately 100 psi to see that the instrumentation was functioning properly and also to check all the loading pads for alignment on the dome surface.

The jack loads were then increased slowly by means of a manual pressure valve up to collapse of the model. The duration of each test from "zero" load up to collapse was approximately three minutes. Photographs were then taken of the collapsed model with the loading system and after the model was carefully removed from the test frame another photograph was taken.

6.7 RESULTS OF STATIC DOME TESTS

Eight model domes, which survived the July, 1962, Small Boy Nevada test, were tested statically as described above. The equivalent uniform radial pressure loads at failure for these models were as follows.

TABLE 6.1
STATIC FAILURE PRESSURES OF THE MODEL DOMES

Model	Chronological Order	Equivalent Uniform failure Pressure	Microconcrete Strength at Test
ND1	5	63.3	4,700 psi
3	6	43.3	4,130
5	7	61.6	5,650
7	8	56.9	4,440
10	3	41.4	no cubes available
11	4	31.4	"
12	1	29.9	"
13	2	47.6	"

The C.E.C. recorder showed a reasonably good agreement between all the load cells. The maximum variation in load from the average jack load on a particular test was generally about 7.0%.

Three model domes which survived the 1961 Canada Tests were used for practice tests in the laboratory. With these and the first few of the Nevada domes that were tested, it was decided that the failure loads were somewhat low due mainly to punching-type failures occurring near the base of the model in the region of boundary moments. To eliminate this situation, oversize steel plates were added under the lower load pads to distribute the load in that region over a greater area and thereby decrease the load concentration. See Figure 6.6 for photograph showing increased load pad size. The first four models tested without these larger pads had an average failure pressure of 37.6 psi. The last four models, using the large pads failed at an average pressure of 56.3 psi.

The failure mechanism on most of the domes tested was generally as expected for a compression-mode type failure - that is, initial yielding near the base (partially fixed support for these models). Figure 6.6 shows a collapsed model with loading system after test and model alone removed from the test frame.

6.8 CONCLUSIONS

With the additional steel pads at the lower load points, a 33% increase in the failure load was obtained. During various tests of the models it was observed that the failure mechanism was always started by one of the lower load pads punching through the shell. It was therefore felt that the load pads were of too small a diameter and were causing stress concentrations in this critical area.

Table 6.2 shows the ultimate membrane strength of the various models and the ultimate strength with bending considered for a fixed support. In both cases, membrane and bending, the ultimate values were obtained from basic shell theory using the ultimate capacity of the reinforced concrete section.

For the cases with the larger load pads, Table 6.2 shows that generally 75-80% of the theoretical bending strength was developed.

The effects of localized bending on the shell surface caused by the discrete point loads may account for some of the reduction in load. Also in applying the elastic shell equations the effective eccentricity was assumed to remain constant up to ultimate. By doing this, one could use the moment-thrust interaction curves to determine the ultimate moment-thrust condition for the model cross-section. The ultimate uniform radial pressure was back figured from this. Assuming constant eccentricity through the inelastic range up to ultimate is highly questionable and thus the tests cannot be expected to show exceedingly good agreement with the calculated membrane-bending case.

TABLE 6.2
EVALUATION OF TEST RESULTS

Model		Ultimate Uniform Radial Pressure (psi)		Static Lab. Tests (psi)
		Pure membrane	Membrane plus Bending	
Large pads	ND 1	132.0	80.0	63.3
	3	135.0	80.9	43.3
	5	129.0	78.2	61.6
	7	117.0	69.6	56.9
Small pads	10	118.0	70.6	41.4
	11	111.0	68.1	31.4
	12	107.1	64.9	29.9
	13	124.5	75.0	47.6

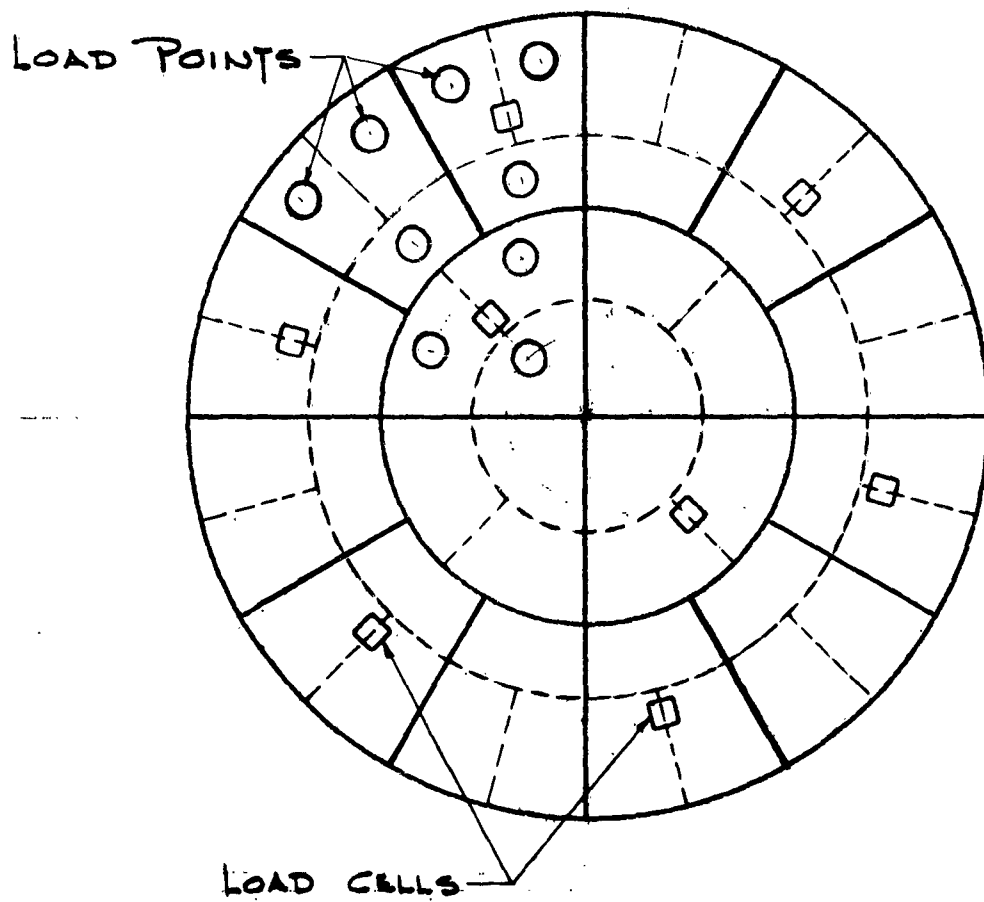


FIGURE 6.1 DISCRETE LOAD LOCATIONS

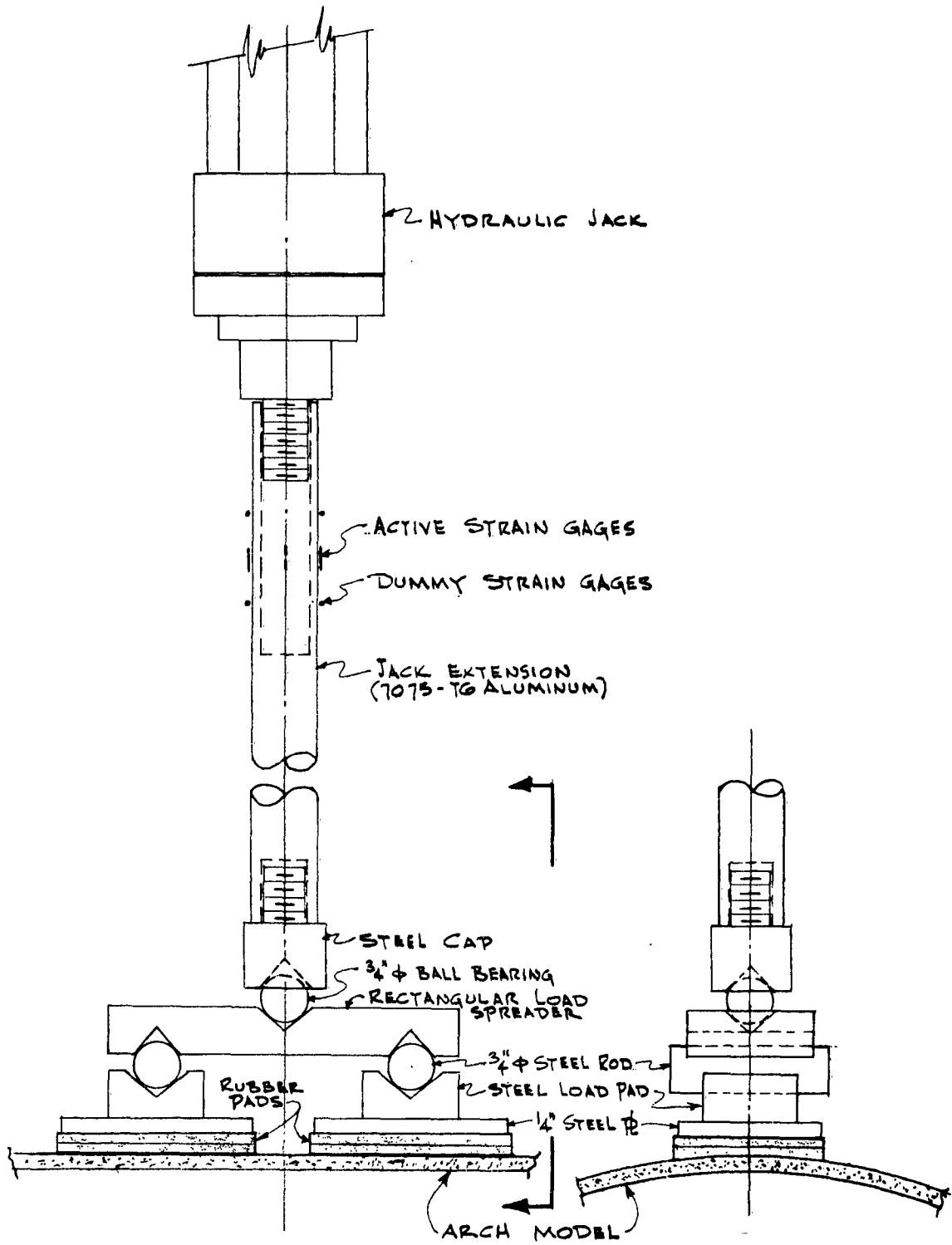


FIGURE 6.2 LOADING SYSTEM

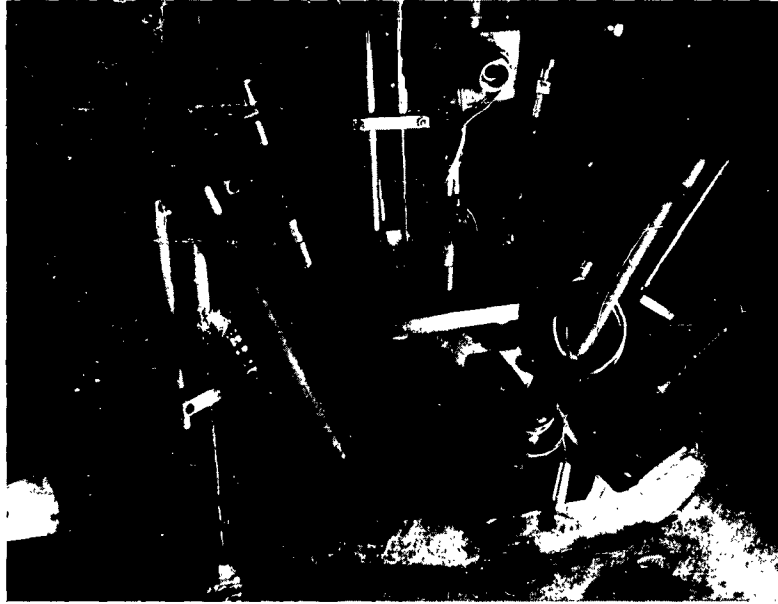
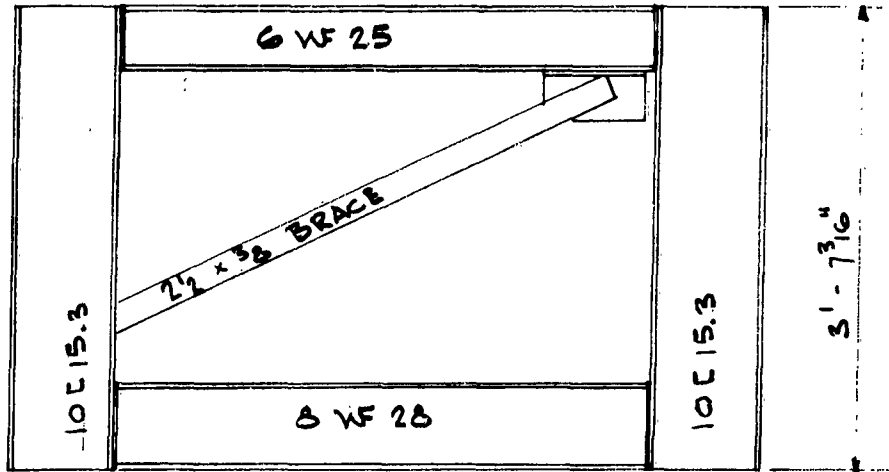


Figure 6.3 Loading System



ELEVATION

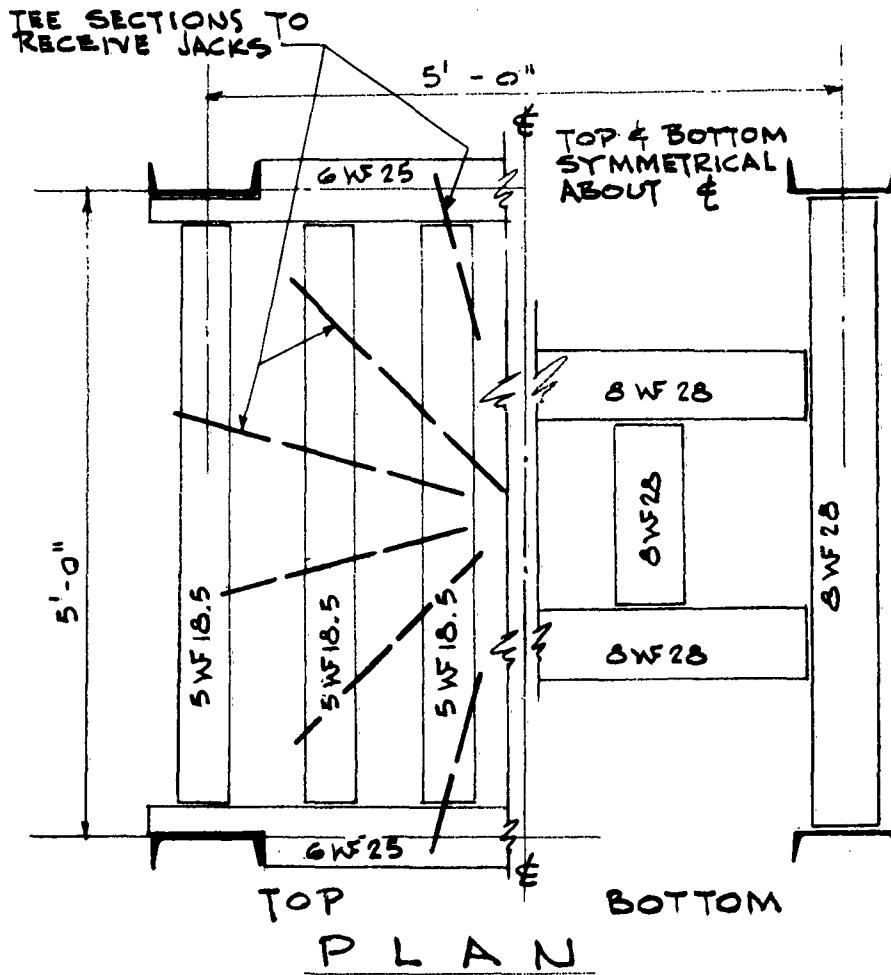


FIGURE 6.4. TEST FRAME

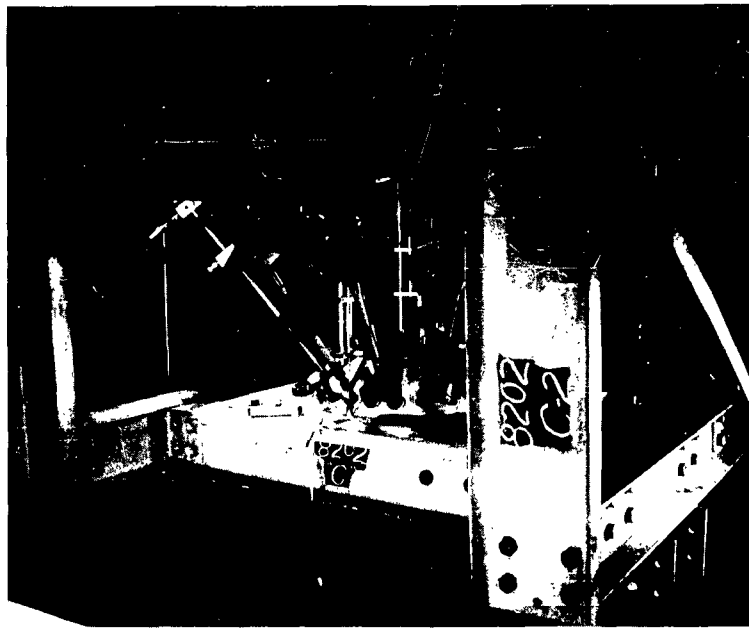
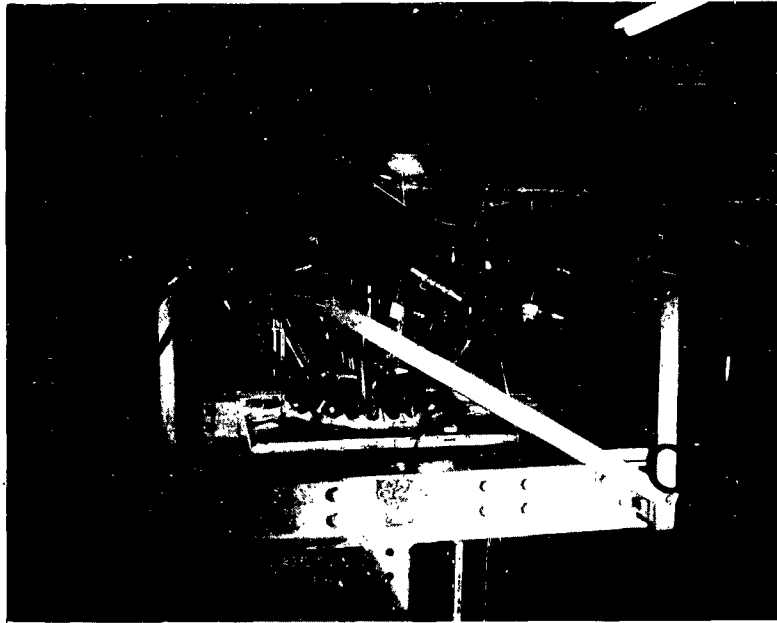


Figure 6.5 Test Frame with Model and Loading System

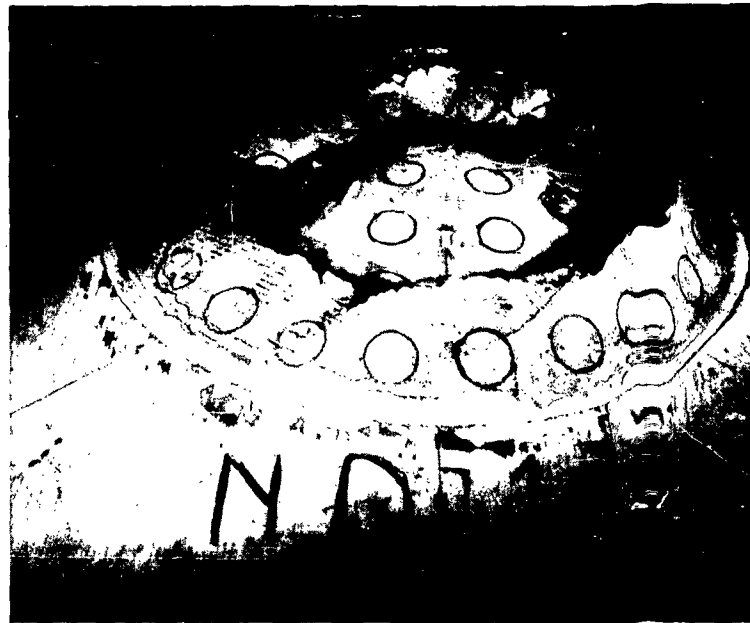


Figure 6.6 Collapsed Model, NDI

CHAPTER 7

CONCLUSIONS

Based upon this project it is concluded that the modeling of structures and their dynamic testing under air blast loading can be quite successful if the proper procedures are followed.

These procedures include selection of the model material in compliance with the similitude restrictions. This requires similarity of the model material stress-strain curve and that of the prototype material. In order to ensure this agreement it was found best to use the same type materials for the models as was used in the prototypes. It was found that a wire reinforced microconcrete works very well as a model of reinforced concrete.

The wire used should be an annealed mild steel, not a high strength carbon wire. Selection should be based upon its stress-strain curve and in particular on its yield stress and ultimate stress. A microconcrete can be produced which is excellent for modeling the behavior of concrete. The parameters of ingredient proportions and sand gradation can be varied to obtain the desired strength and modulus of elasticity and also give the necessary fabrication characteristics such as flow, workability, and low shrinkage.

Blast waves generated by high explosive charges serve very well for simulation of nuclear weapon blast loading. Although the HE charge should be scaled by the cube root law from the mechanical yield of the prototype weapon it may not always be necessary or possible to do so. If the difference between the similitude load-time curve and the model test load time curve is small for the duration of the natural period of the model structure, as was the case in this field test, the change in failure overpressure will be small.

Care in fabrication can result in models whose testing will give reliable data on structural response to dynamic loads. Errors in fabrication will produce models possessing either too low or too high a strength. These experimental errors coupled with others can result

in a scatter of the test data which make interpretation very difficult.

Summing up, it can be said that a carefully planned and executed model study of the response of a structure to air blast loads can give quite reliable results.

REFERENCES

1. Harris, H. G., Pahl, P. J., and Sharma, S. D., "Dynamic Studies of Structures by Means of Models", Technical Report to the Defense Atomic Support Agency, M.I.T., Department of Civil Engineering, 1963.
2. Antebi, J., Smith, H. D., Hansen, R. J., "Study of the Applicability of Models for the Investigation of Air Blast Effects on Structures", Technical Report to the Defense Atomic Support Agency, M.I.T., Department of Civil Engineering, October, 1960.
3. Antebi, J., Utku, S., and Hansen, R. J., "The Response of Shear Walls to Dynamic Loads", DASA-1160, Technical Report to the Defense Atomic Support Agency, M.I.T., Department of Civil Engineering, August, 1960.
4. Kingery, C. N., Keefer, J. H., and Day, S.D., "Surface Air Blast Measurements from a 100-Ton TNT Detonation", Memorandum Report No. 1410, June, 1962, Ballistic Research Laboratories, Aberdeen, Md.
5. Corps of Engineers, U. S. Army, "Design of Structures to Resist the Effects of Atomic Weapons", EM 1110-345-420, January 15, 1960.
6. Morrison, T. G., "Protective Construction, Part III", American Machine and Foundry, AFSWC-TR-59-2, December 1958.
7. A.S.C.E., "Design of Structures to Resist Nuclear Weapons Effects" Manual of Engineering Practice- No. 42, 1961.
8. Norris, et. al., "Structural Design for Dynamic Loads" McGraw-Hill, 1959.
9. Newmark, Hansen and Associates, "Protective Construction Review Guide, Vol. I" Department of Defense, SD-52, June, 1961.
10. Operation Plumbbob, Final Report (CONFIDENTIAL) Defense Atomic Support Agency, Page 42.

**DISTRIBUTION LIST FOR
BLAST & SHOCK
R & D REPORTS**

<u>ADDRESSEE</u>	<u>ARMY</u>	<u>NO. OF CYS.</u>
Chief of Research and Development, D/A, Washington 25, D.C. Attn: Atomic Division		1
Chief of Engineers, D/A, Washington 25, D. C. Attn: ENGOCW-NE		1
ENOTE-E		1
ENGMC-E		1
Commanding General, U. S. Army Materiel Command, Washington, D. C. Attn: AMCRD-DE-N		2
Commandant, Command & General Staff College, Ft. Leavenworth, Kansas, Attn: Archives		1
Commanding General, Aberdeen Proving Ground, Aberdeen, Md. Attn: Director, BRL		1
Commanding General, The Engineer Center, Ft. Belvoir, Va. Attn: Asst. Commandant, Engineer School		1
Director, U. S. Army Research and Development Laboratory Ft. Belvoir, Va. Attn: Chief, Tech. Support Branch		1
Commanding Officer, Picatinny Arsenal, Dover, N. J. Attn: ORDBB-TK		1
Commanding General, USA Electronic R&D Lab., Ft. Monmouth N. J., Attn: Technical Documents Center, Evans Area		1
Director, Waterways Experiment Station, U. S. Army Corps of Engineers, Vicksburg, Mississippi, Attn: Library		1
Director, U. S. Army Corps of Engineers, Nuclear Cratering Group, Livermore, California		1
<u>NAVY</u>		
Chief of Naval Operations, ND, Washington 25, D. C. Attn: OP-75		2
Attn: OP-03EG		1
Chief, Bureau of Yards and Docks, ND, Washington 25, D.C. Attn: Code D-400		1
Attn: Code D-440		1

DISTRIBUTION LIST

(Cont'd.)

<u>ADDRESSEE</u>	<u>NAVY</u>	<u>NO. OF CYS.</u>
Chief of Naval Research, ND, Washington 25, D. C. Attn: Code 811		1
Superintendent, U. S. Naval Postgraduate School, Monterey, California		1
Commanding Officer, U. S. Naval Schools Command, U. S. Naval Station Treasure Island, San Francisco, California		1
Commanding Officer, Nuclear Weapons Training Center, Pacific, Naval Station, North Island, San Diego 35, California		2
Commanding Officer, U. S. Naval Damage Control Training center, Naval Base, Philadelphia 12, Pa. Attn: ABC Defense Course		1
Commander, U. S. Naval Ordnance Laboratory, Silver Spring 19, Maryland, Attn: EA Attn: EU Attn: E		1 1 1
Commander, U. S. Naval Ordnance Test Station, China Lake, California		1
Commanding Officer & Director, U. S. Naval Civil Engineering Laboratory, Port Huenece, Calif., Attn: Code L31		1
Commanding Officer & Director, David W. Taylor Model Basin, Washington 7, D. C., Attn: Library		1
Hq. USAF (AFDRC/NE- Maj. Lowry) ^{AIR FORCE} Washington 25, D. C.		1
Air Force Intelligence Center, Hq. USAF, ACS/I (AFCIN-3K2) Washington 25, D. C.		1
Commander, Air Force Logistics Command, Wright-Patterson AFB, Ohio		2
AFSC, Andrews Air Force Base, Washington 25, D. C., Attn: RDEWA		1
Director, Air University Library, Maxwell AFB, Alabama		2

DISTRIBUTION LIST

(Cont'd.)

<u>ADDRESSEE</u>	<u>AIR FORCE</u>	<u>NO. OF PGS.</u>
AFSWC (SWRS) Kirtland AFB, New Mexico		1
Commandant, Institute of Technology, Wright-Patterson AFB, Ohio, Attn: MCLI-ITRIDL		1
BSD, Norton AFB, California		1
Director, USAF Project RAND, Via: U. S. Air Force Liaison Office, The Rand Corporation, 1700 Main Street, Santa Monica, California		1
Director of Civil Engineering, Hq. USAF, Washington 25, D.C. Attn: APOCE		1
	OTHERS	
Director, Weapons Systems Evaluation Group, OSD, Rm. 1E880, The Pentagon, Washington 25, D. C.		1
Commandant, Armed Forces Staff College, Norfolk 11, Virginia. Attn: Library		1
Commander, Field Command, DASA, Sandia Base, Albuquerque, New Mexico		16
Commander, Field Command, DASA, Sandia Base, Albuquerque, New Mexico, Attn: FCWT		1
Attn: FCTG		1
Chief, Defense Atomic Support Agency, Washington 25, D. C.		5
Officer-in-Charge, U. S. Naval School, Civil Engineering Corps Officers, U. S. Naval Construction Battalion, Port Hueneme, California		1
Los Alamos Scientific Laboratory, P.O. Box 1663, Los Alamos, New Mexico, Attn: Report Librarian (for Dr. A. C. Graves)		1
Chief, Classified Technical Library, Technical Information Service, U. S. Atomic Energy Commission, Washington 25, D. C., Attn: Mrs. Jean O'Leary (for Dr. Paul C. Fine)		1
Dr. Robert J. Hansen, Rm. 1-238, Massachusetts Institute of Technology, 77 Massachusetts Ave. Cambridge, Mass.		1
Chief, Classified Technical Library, Technical Information Service, U. S. Atomic Energy Commission, Washington 25, D.C. Attn: Mrs. Jean O Leary		1

DISTRIBUTION LIST

(Cont'd.)

<u>ADDRESSEE</u>	<u>OTHERS (Cont'd.)</u>	<u>NO. OF PGS.</u>
Dr. Bruce G. Johnston, The University of Michigan, University Research Security Office, Lobby 1, East Engineering Bldg., Ann Arbor, Michigan		1
Sandia Corporation, Sandia Base, Albuquerque, New Mexico, Attn: Classified Document Division (for Dr. M. L. Merritt)		1
Dr. Nathan M. Newmark, University of Illinois, Rm. 207, Talbot Laboratory, Urbana, Illinois.		1
Commander, ASTIA, Arlington Hall Station, Arlington 12, Virginia, Attn: TIPDR		15
Holmes & Narver, Inc., AEC Facilities Division, 849 S. Broadway Los Angeles 14, California Attn: Mr. Frank Galbreth		1
Professor Robert V. Whitman, Massachusetts Institute of Technology, Rm. 1-343, Cambridge 39, Mass.		1
Professor J. Neils Thompson, University of Texas, Structural Mechanics Research Laboratory, Austin, Texas		1
Dr. Neidhardt, General American Transportation Corporation, 7501 N. Natchez Avenue, Niles, Illinois		1
Mr. Sherwood Smith, Roland F. Beers, Inc., 2520 Oakville, Alexandria, Va.		1
Paul Weidlinger, Consulting Engineer, 770 Lexington Ave., New York 21, New York, Attn: Dr. M. Baron		1
Mr. A. Weideman, Armour Research Foundation, 10 West 35th St. Chicago 16, Illinois		1